P-06-04

# Oskarshamn site investigation

# Fracture mineralogy of the Götemar granite

## Results from drill cores KKR01, KKR02 and KKR03

Henrik Drake
Department of Geology, Earth Sciences Centre,
Göteborg University

Eva-Lena Tullborg, Terralogica AB

January 2006

**Svensk Kärnbränslehantering AB**
Swedish Nuclear Fuel
and Waste Management Co
Box 5864
SE-102 40 Stockholm Sweden
Tel 08-459 84 00
+46 8 459 84 00
Fax 08-661 57 19
+46 8 661 57 19

ISSN 1651-4416
SKB P-06-04

# Oskarshamn site investigation

# Fracture mineralogy of the Götemar granite

## Results from drill cores KKR01, KKR02 and KKR03

Henrik Drake
Department of Geology, Earth Sciences Centre,
Göteborg University

Eva-Lena Tullborg, Terralogica AB

January 2006

*Keywords:* Fracture minerals, Götemar, South-eastern Sweden, Anorogenic granite, Calcite, Pyrite, Fluorite, Stable isotopes, SEM-EDS.

# Abstract

Fracture mineralogical studies have been carried out on three deep cored boreholes, KKR01, KKR02 and KKR03, drilled in the 1970's, in the Götemar granite as part of SKB's site investigation programme. The Götemar granite is an anorogenic granite massif that crops out some kilometres north of the SKB candidate area at Simpevarp/Laxemar, situated in Precambrian crystalline rocks belonging to the Transscandinavian Igneous Belt (TIB). Thin sections of open and sealed fractures and fracture surface samples from open fractures have been analysed using petrographic microscope and scanning electron microscope (SEM-EDS). Calcite samples have been analysed for $\delta^{18}O$, $\delta^{13}C$ and $^{87}Sr/^{86}Sr$. Fluorite samples have been analysed for $^{87}Sr/^{86}Sr$. Pyrite samples have been analysed for $\delta^{34}S$. Two additional thin sections of sandstone dykes from Kråkemåla quarry #2 are also included in the study. The aim of this study has been to: 1) identify, characterize and establish a sequence of fracture filling generations that can add to the geological description of the site 2) compare and correlate Götemar fracture fillings to fracture filling generations from adjacent TIB-rocks from Simpevarp/Laxemar /Drake and Tullborg 2004, 2005/, to provide relative dating of these fillings and 3) to give input to the palaeohydrogeological interpretations of the area.

The results from this study show that the fractures from the Götemar granite host fillings of fewer generations than in the adjacent TIB-rocks. The relative relations between different fracture-filling parageneses have been difficult to establish since there exist few cross-cutting relations of different fracture generations and the fractures are seldom re-activated. It has however been possible to distinguish two major fracture filling generations. The probably earliest formed generation is a breccia-sealing that appears in different varieties. The latest formed fracture filling generation consists of mainly calcite, fluorite, quartz, chlorite, pyrite and additionally e.g. galena, hematite, barite, sphalerite, U-silicate, REE-carbonate, chalcopyrite and Cu-oxide. The early formed breccia-sealing is commonly made up of albite, muscovite, quartz, chlorite and subordinately of hematite, K-feldspar, fluorite and possibly illite. The minerals in this generation reflect the wall rock chemistry, rich in K and Na, and a lack of calcium-bearing minerals, which is in contradiction to fracture fillings in nearby TIB-rocks, which are characterized by early formed Ca-rich fillings, epidote, prehnite and laumontite. Since the earliest formed fracture fillings in the TIB-rocks and in the Götemar granite probably are precipitated from locally derived fluids, it is complicated to correlate these.

The calcite-fluorite fillings are presumed to be formed subsequent to the breccia-sealings, and fluorite from this generation has been dated to 405 ± 27 Ma /Sundblad et al. 2004/. These fillings also seal fractures that cross-cut sandstone of presumed Cambrian age. $\delta^{13}C$ and $\delta^{18}O$ values of calcite from this generation resemble to late formed calcite from Simpevarp, Laxemar and Äspö /Tullborg 1997, Wallin and Peterman 1999, Bath et al. 2000, Drake and Tullborg 2004, 2006a/. The paragenesis of this calcite-fluorite generation is very similar to the late formed calcite-fluorite fillings in Simpevarp and Laxemar. The $^{87}Sr/^{86}Sr$ values of the Götemar calcites are homogeneous and slightly higher than most of the $^{87}Sr/^{86}Sr$ values from Simpevarp and Laxemar calcites /Drake and Tullborg 2004, 2006a/, which may reflect different $^{87}Sr/^{86}Sr$-ratios of the wall rock. Highly enriched $\delta^{34}S$-values of pyrite and very low $\delta^{13}C$-values of calcite are occasionally observed in this generation, as well as in the related TIB-fracture fillings, and suggest biogenic activity (microbial sulphate reduction) in the ground water aquifer, resulting in disequilibrium in situ. $^{87}Sr/^{86}Sr$-ratios in fluorite are generally highly enriched compared to associated calcite.

# Sammanfattning

Sprickmineralogiska studier av tre djupa kärnborrhål, borrade på 1970-talet i Götemar graniten, har utförts inom ramen för SKB's platsundersökningar. Götemargraniten är en anorogen granit som är belägen några kilometer norr om platsundersökningsområdet Simpevarp/Laxemar, som i sin tur är beläget i pre-kambrisk kristallin berggrund tillhörande det Transskandinaviska Magmatiska Bältet (TMB). Tunnslip från öppna och läkta sprickor och ytprover från sprickytor i öppna sprickor har analyserats med petrografiskt mikroskop och svepelektronmikroskop (SEM-EDS). $\delta^{18}O$-, $\delta^{13}C$- och $^{87}Sr/^{86}Sr$-halter i kalcit, $^{87}Sr/^{86}Sr$-halter i fluorit och $\delta^{34}S$-halter i pyrit har analyserats med masspektrometer. Tunnslip från två sandstensgångar från Kråkemåla stenbrott nr 2 har också undersökts.

Syftet med studien har varit att: 1) identifiera, karaktärisera och konstruera en sprickfyllnads-sekvens bestående av olika sprickfyllnadsgenerationer som skall adderas till den geologiska modellen för området 2) jämföra och korrelera sprickfyllnader från Götemar graniten med sprickfyllnadsgenerationer från närliggande TMB-bergarter från Simpevarp-Laxemar /Drake and Tullborg 2004, 2005/, för att datera dessa relativt och 3) ge information om palaeohydrogeologiska förhållanden.

Resultaten från denna studie antyder att sprickorna i Götemar graniten innehåller färre generationer av sprickmineral än vad de närliggande TMB-bergarterna gör. Inbördes relationer mellan olika sprickmineralgenerationer i Götemar graniten är svåra att urskilja då klippande sprickor av olika generationer och reaktivering av sprickor är ovanliga. Det har dock varit möjligt att urskilja två huvudgenerationer, en breccia-läkning med varierande mineralinnehåll och en troligen senare bildad fyllning bestående av främst kalcit, fluorit, kvarts, klorit, pyrit och i mindre utsträckning t ex blyglans, hematit, zinkblände, baryt, U-silikat, REE-karbonat, kopparkis, adularia och Cu-oxid.

De tidigt bildade breccia-läkningarna består mestadels av albit, muskovit, kvarts, klorit och till en mindre del av hämatit, kalifältspat, fluorit och möjligen illit. Mineralen i denna generation avspeglar Götemargranitens kemi, med hög andel K och Na, i motsats till de tidigast bildade sprickfyllningarna i närliggande TMB-bergarter som vanligen består av Ca-silikat; epidot, prehnit och laumontit. Eftersom fluiderna som avsatt de tidigaste sprickmineralgenerationerna i både Götemar graniten och TMB-bergarterna verkar avspegla den lokala bergartskemin är det svårt att korrelera sprickmineralgenerationerna med varandra.

De kalcit- och fluoritförande fyllningarna är troligen bildade senare än breccia-läkningarna och har daterats till 405 ± 27 Ma /Sundblad et al. 2004/. Dessa fyllningar finns även i sprickor som klipper sandsten med en trolig kambrisk ålder. $\delta^{13}C$- och $\delta^{18}O$-värden för kalcit från denna generation är lika värden från relativt sent bildade kalciter som beskrivits tidigare från Simpevarp, Laxemar och Äspö /Tullborg 1997, Wallin and Peterman 1999, Bath et al. 2000, Drake and Tullborg 2004, 2006a/. Paragenesen i denna generation är mycket lik den sent bildade kalcit-fluoritgenerationen från Simpevarp och Laxemar. Kalcit från Götemar har homogena $^{87}Sr/^{86}Sr$-värden som är något högre än de flesta $^{87}Sr/^{86}Sr$-värden i kalciter från Simpevarp och Laxemar /Drake and Tullborg 2004, 2006a/. Detta kan dock bero på influens från sidobergets $^{87}Sr/^{86}Sr$-kvoter. Höga $\delta^{34}S$-värden i pyrit och mycket låga $\delta^{13}C$-värden i kalcit har observerats i ett par prover i denna generation och i relaterade sprickläkningar från TMB, vilket antyder biogen aktivitet i form av mikrobiell sulfatreduktion i grundvattenakvifären. $^{87}Sr/^{86}Sr$-värden i fluorit är generellt höga jämfört med relaterad kalcit.

# Contents

# 1 Introduction

The Swedish Nuclear Fuel and Waste Management Company (SKB) is currently carrying out site investigations in the Simpevarp/Laxemar area in the Oskarshamn region. Three drill cores from previous investigations, KKR01, KKR02 and KKR03 from Kråkemåla (Figure 1-1) have been samples for detailed studies of fracture mineralogy and isotope geochemistry. These boreholes are drilled into the Götemar granite which crops out some kilometres north of the SKB site investigation area at Simpevarp/Laxemar. Two additional samples of sandstone dykes from Kråkemåla quarry 2 are also included in this study. The results have been compared to the detailed fracture filling studies of drill-cores KSH01, KSH03, KLX02, KAS 04, KA1755A /Drake and Tullborg 2004, 2005, 2006a/, KLX03, KLX04, KLX05 and KLX06 /Drake and Tullborg, in manuscript/, which are drilled into rocks of the Transscandinavian Igneous Belt (TIB), surrounding the Götemar intrusion. Drill cores KSH01, KSH03, KLX03, KLX04, KLX05 and KLX06 were drilled with triple tube technique which generally results in better preservation of the fracture coatings than the conventional drilling technique used for drill cores KKR01, KKR02, KKR03, KLX02, KAS04 and KA1755A.

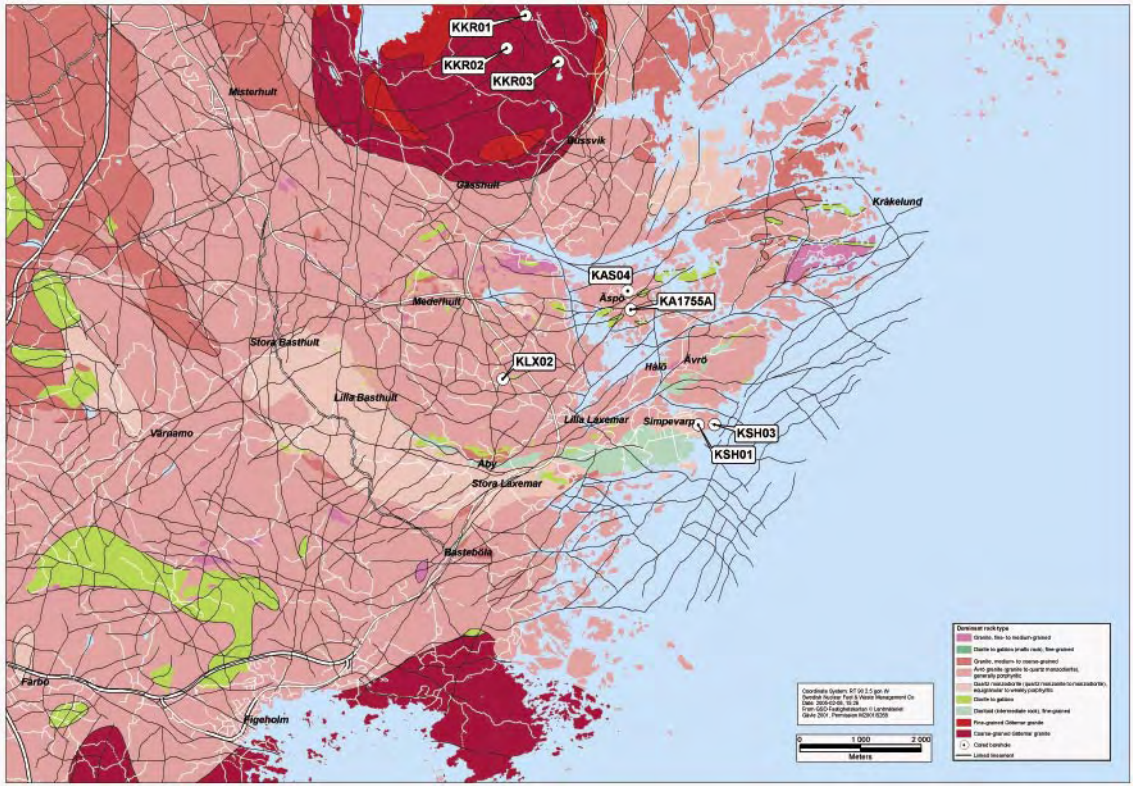


***Figure 1-1.*** *Geological map showing the surface-locations of bore holes KKR01, KKR02 and KKR03 and the Götemar granite (northern part of map). The Uthammar granite is visible in the southern part of the map. Locations of bore holes KSH01, KSH03, KLX02, KAS04 and KA1755A are also shown.*

A total number of 34 samples from which 7 thin-sections and 16 fracture surface samples from open fractures with fracture coatings were prepared, have been analysed using petrographic microscope, stereomicroscope and scanning electron microscope (SEM). Fourteen calcite samples have been analysed for $\delta^{18}O/\delta^{13}C$ and five samples have been analysed for $^{87}Sr/^{86}Sr$. Five fluorite samples have been analysed for $^{87}Sr/^{86}Sr$ and four pyrite samples for $\delta^{34}S$.

The work was carried out in accordance with activity plan SKB PS 400-04-018. In Table 1-1 controlling documents for performing this activity are listed. Both activity plan and method descriptions are SKB's internal controlling documents.

**Table 1-1. Controlling documents for the performance of the activity**

| **Activity plan** | **Number** | **Version** |
|---|---|---|
| Sprickmineralogiska undersökningar | AP PS 400-04-018 | 1.0 |
| **Method descriptions** | **Number** | **Version** |
| Sprickmineralogi | SKB MD 144.000 | 1.0 |

# 2 Objective and scope

The aim of this study is to obtain a detailed description, including mineralogy, geochemistry and isotopic composition, of the most characteristic fracture fillings in the Götemar granite. This information will be compared to information of the fracture fillings in the TIB-rocks /Tullborg 1988, 1997, Drake and Tullborg 2004, 2005, 2006a/, surrounding the younger Götemar intrusion. An important part of this comparison is to determine if the fracture fillings in the TIB-rocks and in the Götemar granite are similar and can be related to the same events. The fracture mineralogy gives indications of the fluids from which the fracture minerals precipitated. Similar mineralogy, chemistry and isotope composition of the fracture fillings in the Götemar granite and the TIB-rocks will thus indicate relative timing of the fracture minerals in the TIB-rocks. Furthermore, comparisons of fracture mineralogy and trace element composition in the minerals between the Götemar granite and the TIB-rocks will give indications of how far the fluids moved through the fractures before precipitation; if the fracture mineralogy reflects the local country rock composition or if the fracture fillings are similar throughout the region.

This study constitutes a part of a Fil.Lic. project at the Department of Geology, Earth Sciences Centre, Göteborg University.

# 3 Geological background

## 3.1 Götemar granite

The Götemar granite crops out some kilometres north of the site investigation candidate area. It is an anorogenic granite related to the Uthammar granite which crops out some kilometres south of the candidate area. Both of these intrusions are intruding granitoids belonging to the Transscandinavian Igneous Belt (TIB) /Gaal and Gorbatschev 1987/. The southern contact between TIB and the Götemar granite is thought to be dipping towards the candidate area and the Götemar granite outcrops are thought to represent the upper part of a diapiric intrusion cf Figure 11-1 in /SKB 2005/. The Götemar massif is nearly circular in outline with a diameter of 5 km and is presumed to be emplaced as a crystallized mush with high volatile content at subvolcanic level /Kresten and Chyssler 1976/. The contacts with the surrounding TIB-granite are generally sharp and well defined and the TIB-granite is porous and altered in a greisen-like manner 0–25 m from the contact /Kresten and Chyssler 1976/.

Earlier studies of the Götemar granite have been carried out by e.g. /Kresten and Chyssler 1976, Åberg 1978, Åberg et al. 1984, Smellie and Stuckless 1985/. Rb-Sr, U-Pb and K-Ar dating of the granite yielded ages of 1,350–1,400 Ma /Åberg 1978, Åberg et al. 1984/ and U-Pb dating with zircons gave an age of 1,452 +11/–9 Ma /Åhäll 2001/. U-Pb dating with zircons from the Uthammar granite yielded an age of 1,441 +5/–3 Ma /Åhäll 2001/. K-Ar ages reveal that the temperatures have probably not exceeded 300°C since the granite crystallised /Åberg 1978, Smellie and Stuckless 1985/. Hydrous solutions have however passed through the rock and reacted with it at more moderate temperatures /Smellie and Stuckless 1985/.

The Götemar granite mainly consists of coarse-grained homogeneous alkali feldspar granite with subordinate fine-grained varieties /Åberg et al. 1984/. According to /Kresten and Chyssler 1976/ the Götemar granite has four principle textural varieties, despite the overall relatively uniform mineralogy and major element chemistry. The granite is highly differentiated and composed of K-feldspar-albite (as mesoperthite), quartz and minor amounts of biotite, muscovite and magnetite with fluorite, zircon, monazite, apatite, titanite and topaz as accessory minerals /Kresten and Chyssler 1976, Åberg 1978/. The chemical composition of the Götemar granite ranges from alkali granite and syenite and the silica, alkali and fluorine (average 0.43% F) contents are fairly high while the iron and magnesium contents are low and the calcium values are very low (0.02 to 0.6% CaO) /Kresten and Chyssler 1976/. In the adjacent TIB-granites, the fluorine contents are much lower (0.05 to 0.23% F) /Drake and Tullborg 2006b/.

Alteration of the granite has been site specific and had no marked effect on major-element chemistry, other than small effects on alkalis /Smellie and Stuckless 1985/. Isotopic analyses reveal open-system behaviours for Pb and U, and indicate that hydrothermal alteration may have taken place within the range of 420 ± 171 Ma /Smellie and Stuckless 1985/.

Radial, tangential and flat-lying joints dominate in the massif and these persist as far as 500 m into the adjacent TIB-granites /Kresten and Chyssler 1976/.

### 3.1.1 Götemar fracture fillings

Fracture coatings of chlorite, quartz, fluorite, mica, pyrite, chalcopyrite and galena as well as sandstone dykes with fluorite cement were reported by /Kresten and Chyssler 1976/.

Studies of the fluorite-calcite-galena bearing fractures in the counties of Blekinge and Kalmar, including the Götemar granite have been carried out by /Alm and Sundblad 2002/. Occurrences of fluorite-calcite bearing fractures along the Baltic Sea coast of south-eastern Sweden have earlier been described by e.g. /Carlsson and Holmqvist 1968, Sollien 1999/. These occur in the Precambrian crystalline basement and are often found in some association with Cambrian sandstone dykes, related to the sub-Cambrian peneplane e.g. /Alm and Sundblad 2002/. They are most frequent along the Småland coast and on the islands of Åland. In the Oskarshamn-Västervik region, these fractures are filled with sandstone material and may be of Cambrian age. They are mainly oriented in N-S to NNE and ENE and follow the orientation of the fracture sets in the basement /Nordenskjöld 1944, Sundblad 2000/. The sandstone dykes in the Äspö area are sub-vertical, have a fairly consistent trend (N35°E) and range in thickness from a few tens of centimetres to a few millimetres /Röshoff and Cosgrove 2002/. The quartz and feldspar grains are rounded to angular. The colour varies within a single dyke from greyish, brownish, yellowish to greenish /Röshoff and Cosgrove 2002/.

The sandstone dykes in the Götemar granite have recently been studied by /Röshoff and Cosgrove 2002/, who claims that a majority of the sandstone dykes in the Oskarshamn-Västervik region were formed by forceful injection by external fluid pressure into the basement in pre-existing fractures and presumably also in fractures induced by the forceful injection. This is in contradiction to earlier studies (e.g. /Kresten and Chyssler 1976, Alm and Sundblad 2002/, concluding that the fractures were filled passively. /Röshoff and Cosgrove 2002/ describe the texture of the sandstone dykes in the Götemar granite as made up of well-rounded clasts of quartz that generally become more angular and fine-grained towards the wall rock contact. The latter features and the presence of angular K-feldspar crystals in the sandstone that are interpreted to be fragments plucked from the wall rock are indications of forceful injection /Röshoff and Cosgrove 2002/, and references therein).

The fluorite-calcite-galena bearing fractures in the Götemar granite have been dated to 405 ± 27 Ma, with Sm/Nd on fluorite /Sundblad et al. 2004/. These fillings also cut through the “Cambrian” sandstone-dykes and primary porous sandstone-dykes have sometimes been filled with fluorite as cement after consolidation of the sandstone /Alm and Sundblad 2002, Röshoff and Cosgrove 2002/.

Fluid inclusion data indicate depositional temperatures for the fluorite-calcite-galena fillings at 80–160°C, which implies that the fluorine probably only is leached from free fluorite in the wall rock and not from other F-bearing minerals like biotite /Alm and Sundblad 2002/.

## 3.2 Fracture mineralogy in the Simpevarp-Laxemar area

Earlier studies of the fracture mineralogy in the TIB-rocks in the vicinity of the Götemar granite have been carried out by e.g. /Tullborg 1988, 1997, Drake and Tullborg 2004, 2005, 2006a/. The fracture mineralogical model compiled from investigations of the drill cores KSH01, KSH03, KLX02, KLX03, KLX04, KLX05, KLX06, KAS 04 and KA17755A /Drake and Tullborg 2006a/ is shown in the appendix.

# 4 The drill cores

The drill cores are made up of Götemar granite of relatively homogeneous composition. The major varieties are granite of different grain-size. The coarse-grained variety is much more common than the fine-grained, aplitic variety. The description of the drill cores below are from mapping protocols of The Geological Survey of Sweden (SGU). Different nomenclature has been used for the different drill-cores, where “red granite” and “red, medium- to coarse-grained granite” describes the coarse-grained variety of the Götemar granite and “red aplitic granite” and “greyish red aplitic granite” describe the fine-grained variety.

## 4.1 KKR01

The length of the borehole is 506.15 m and was drilled in 1977. The main rock types are “red granite” and “red aplitic granite” in order of abundance. More extensive sections of altered and brecciated granite is found at 11 to 12 m, at several depths between 141 and 152 m, at several depths between 165 and 174 m, at 223.50 to 224.20 m, at 235.20 to 236.90 m, at 245.90 to 247.20 m, 294.00 to 298.00 m, 312.00 to 317.00 m, and 404.00 to 405.00 m.

## 4.2 KKR02

The length of the borehole is 602.40 m and was drilled in 1977. The main rock types are “red granite” and “red aplitic granite” in order of abundance. Altered and brecciated granite is found at 34.50 to 34.65 m, 83.00 to 84.00 m, and at several depths between 286.90 and 366.60 m.

## 4.3 KKR03

The length of the borehole is 761.40 m which gives a vertical depth of 580 m since it was drilled with an inclination of 50 º to the north. The borehole was drilled in 1978. The main rock types are “red, medium- to coarse-grained granite” with small amounts of “greyish red aplitic granite” in order of abundance. A smaller section of heavily altered granite is also present at 172.20 to 172.65 m.

# 5 Equipment

## 5.1 Description of equipment

The following equipment was used in the fracture mineralogy investigations of drill cores KKR01, KKR02 and KKR03.

- Scanning electron microscope (Zeiss DSM 940) with EDS (Oxford Instruments Link).
- Microscopes (Leica DMRXP and Leica DMLP).
- Stereo microscope (Leica MZ12).
- Microscope camera (JVC TK-1280E).
- Digital camera (Konica Revio KD-420Z).
- Stone cutter.
- Magnifying lens – 10x.
- Scanner (Epson 3200) and Polaroid filters.
- Computer software, e.g. Corel Draw 11, Microsoft Word, Microsoft Excel, Link ISIS.
- Mass-spectrometer.

All of the equipment listed above is property of the Earth Sciences Centre, Göteborg University, SKB or the authors.

External laboratory equipment was used for $^{87}Sr$-$^{86}Sr$ analysis and $\delta^{34}S$-analysis.

# 6 Execution

## 6.1 Sample collection

Drill core samples suitable for fracture mineral investigations were collected from drill cores KKR01, KKR02 and KKR03 at the SKB drill core store in Krisslinge close to Uppsala. The collection of the samples were scattered throughout the drill cores and the length of the samples ranges from 3 to 20 cm. No statistical approach was considered in the sampling procedure, instead suitable samples were selected. Two hand-samples of sandstone were collected from Kråkemåla quarry 2. Sampling was focused on comparison between adjacent fracture-filling generations in TIB-rocks and to find cross-cutting relations of different fracture-filling generations.

BIPS-work has not been conducted in the bore holes and no information of the strike or dip of the studied fractures can thus be used. In contrast to the drillings in Simpevarp and Laxemar the bore holes were not drilled with triple-tube drilling. The drill core quality is thus lower for the drill cores investigated in this study. This lower quality especially affects clay minerals and other minerals in open fractures, which may be destroyed or even flushed away.

## 6.2 Sample preparation and analyses

### 6.2.1 Thin sections and fracture surface samples

The samples were first photographed and sawed. Then 7 thin sections and 16 surface samples (Table 6-1) were prepared from sealed and open fractures. Thin section preparation was carried out at the Earth Sciences Centre, Göteborg University by Ali Firoozan and by Kjell Helge, Minoprep AB, respectively. The thicknesses of the thin sections were 100 µm (2 samples) and 30 µm (5 samples). The thin sections and the surface samples were scanned with Epson 3200 scanner, using Polaroid filters for the thin sections, in order to optimize SEM-investigations. The prepared samples were initially examined with transmissive microscope (thin sections) and stereo microscope (surface samples).

The thin sections and surface samples were examined in detail and analysed with an Oxford Instruments energy dispersive system mounted on a Zeiss DSM 940 SEM at the Earth Sciences Centre, Göteborg University, Sweden. Polished thin-sections were coated with carbon and surface samples were coated with gold for electron conductivity. The acceleration voltage was 25 kV, the working distance 24 mm (18 mm for surface samples) and the specimen current was about 0.7nA. The instrument was calibrated at least twice every hour using a cobalt standard. ZAF calculations were maintained by an on-line LINK ISIS computer system. These quantitative analyses give reliable mineral compositions but $Fe^{2+}$ and $Fe^{3+}$ are not distinguished, neither is the $H_2O$ content calculated. Detection limits for major elements are higher than 0.1 oxide %, except for $Na_2O$ with a detection limit of 0.3%.

### 6.2.2 Calcite and fluorite analyses

The stable carbon and oxygen isotope analyses carried out at the Earth Sciences Centre, Göteborg University, on 14 calcite samples (Table 6-1) were made accordingly: Samples, usually between 150 and 250 µg each, were roasted in vacuum for 30 minutes at 400°C to

remove possible organic material and moisture. Thereafter, the samples were analysed using a VG Prism Series II mass spectrometer with a VG Isocarb preparation system on line. In the preparation system each sample was reacted with 100% phosphoric acid at 90°C for 10 minutes, whereupon the released $CO_2$ gas was analysed in the mass spectrometer. All isotope results are reported as δ per mil relative to the Vienna Pee Dee Belemnite (VPDB) standard. The analysing system is calibrated to the PDB scale via NBS-19.

For the Sr isotope analyses about 30 to 40 mg of the 5 calcite samples (Table 6-1) were transferred to 2 ml centrifuge tubes, added 200 µl 0.2 M HCl, and shaken. The samples were let to react for 10 minutes while shaken in order to release the $CO_2$ gas. If not completely dissolved 20 µl 2 M HCl is added once or twice until most of the calcite has been decomposed. The fluorite samples were finely ground in an agate mortar and transferred to a Savillex teflon beaker with lid. A few ml of suprapure $HNO_3$ was added, the lid screwed loosely on and the beaker was put onto a hotplate at low temperature for 48 hours. During this time the beaker was shaken several times in order to leach the fluorite as good as possible.

All the samples were centrifuged for about 4 minutes and the liquids transferred to new clean centrifuge tubes by use of a pipette. The centrifuge tubes were put in an Al-block on a hotplate and evaporated to dryness. To avoid disturbances in measuring the isotopic composition strontium had to be separated from other elements present in the sample. After evaporation to dryness the samples were dissolved in 200 µl ultrapure 3M $HNO_3$, centrifuged and loaded onto ion-exchange columns packed with a Sr-Spec crown-ether resin from EIChrom, which retained Sr and allowed most other elements to pass. After rinsing out the remaining unwanted elements from the columns, strontium was collected with ultrapure water (Millipore). The collected Sr- fractions were then evaporated to dryness and loaded on pre-gassed Re filaments on a turret holding 12 samples and 1 NIST/NBS 987 Sr standard. The isotopic composition of Sr was determined by thermal ionization mass spectrometry (TIMS) on a Finnigan MAT 261 with a precision of about 20 ppm and a Sr blank of 50–100 pg. The $^{87}Sr/^{86}Sr$ ratio of the carbonate analysis are monitored by analysing one NIST/NBS SRM 987 Sr standard, for each turret of 12 samples, and the standard has a recommended $^{87}Sr/^{86}Sr$ value of 0.710248. The presented results are not corrected to the NBS 987 recommended value but given together with the specific measured NBS 987 value for the relevant turret. The Sr analyses were carried out by Göran Åberg at the Institute for Energy Technology, Norway.

### 6.2.3 Pyrite analysis

Four samples of euhedral pyrite crystals from fracture surfaces (Table 6-1) have been analysed for their stable-isotope composition, expressed as $\delta^{34}S$. The pyrite crystals were scraped of the fracture surface with a knife. Bigger crystals were handpicked from the surface with a pair of tweezers. The analyses were carried out at the Scottish Universities Environmental Research Centre, Glasgow by Professor Tony Fallick. Sulphur dioxide was liberated from sulphides following the method of /Robinson and Kusakabe 1975/, whereby samples were combusted at 1,070°C for 25 minutes in the presence of excess $Cu_2O$. A high temperature furnace containing pure copper ensured that any sulphur trioxide in the combustion products was reduced to $SO_2$. Sulphur dioxide was separated from excess oxygen and the other combustion products by standard vacuum line techniques, and the purified gas analysed for $^{34}S/^{32}S$ ratio on a dual-inlet Micromass SIRA2 multiple-collector mass spectrometer. Reproducibility of calibrated standards is ± 0.2‰ at one sigma and data are reported in the delta notation relative to V-CDT.

**Table 6-1. Sample names, sample types and analyses (1 = calcite, 2 = fluorite, 3 = pyrite).**

| Sample (m) | Thin section | Surface sample | $\delta^{13}C$ / $\delta^{18}O$[1] | $^{87}Sr/^{86}Sr$[1,2] | $\delta^{34}S$[3] |
|---|---|---|---|---|---|
| KKR01 – 153.40–153.50 | | x | | | |
| KKR01 – 157.30–157.45 | | x | | | |
| KKR01 – 163.70–163.75 | | x | | | |
| KKR01 – 492.75–492.80 | x | | | | |
| KKR02 – 23.12–23.25 | | x | x | | |
| KKR02 – 48.95–49.00 | | | xx | x[1] | |
| KKR02 – 95.75–95.95 | | x | | | |
| KKR02 – 159.92–159.95 | | x | | | |
| KKR02 – 171.52–171.61 | | x | x | | |
| KKR02 – 213.42–213.55 | | | x | | x |
| KKR02 – 213.90–214.00 | | | x | x[1], x[2] | x |
| KKR02 – 236.69–236.84 | | x | x | x[1], x[2] | |
| KKR02 – 258.24–258.41 | | x | | | |
| KKR02 – 367.58–367.73 | | x | | | |
| KKR03 – 52.25–52.37 | x | | x | x[1], x[2] | |
| KKR03 – 54.83–54.86 | | x | xx | x[2] | x |
| KKR03 – 75.20–75.30 | | x | x | x[2] | x |
| KKR03 – 251.83–251.85 | x | | | | |
| KKR03 – 258.23–258.34 | | x | | | |
| KKR03 – 336.66–336.72 | | x | | | |
| KKR03 – 389.11–389.13 | | x | x | | |
| KKR03 – 459.02–459.12 | | | x | | |
| KKR03 – 539.04–539.12 | | x | x | x1 | |
| KKR03 – 651.75–651.79 | x | | | | |
| KKR03 – 733.55–733.58 | x | | | | |
| Sandstone1 | x | | | | |
| Sandstone2 | x | | | | |
| Number of samples | 7 | 16 | 14 | 51.52 | 4 |

# 7 Results and discussion

Re-activation and cross-cutting fractures are rare in samples from the Götemar granite. Some patterns have been distinguished, concerning the fracture sealing; e.g. fluorite is often coating fracture walls and paragenetic calcite is more common in the centre of the sealed fillings and has precipitated on top of fluorite in open fractures. This pattern is visible in hand sample, while microscope or handlens is usually necessary to identify the most fine-grained crystals of e.g. chlorite, pyrite and galena that are growing on the surface of calcite and fluorite crystals.

Roughly, two generations of fracture fillings can be distinguished.

1. Breccia-sealings consisting of albite, muscovite, quartz, chlorite (Fe-rich), (hematite), (illite), (K-feldspar), (fluorite).
2. Calcite-fluorite-rich fillings, consisting of calcite, fluorite, quartz, chlorite (Fe-rich + ML-clay), pyrite and galena. Occasionally, hematite, sphalerite, barite, U-silicate, REE-carbonate, Cu-oxide, adularia, apatite, chalcopyrite and wolframite are present.

Both of these two generations might be made up of sub-generations possibly formed at different events. The calcite-fluorite fillings have similar features in most of the samples and are generally presumed to be formed at one single event. However, the more rare minerals in these fillings appear randomly. The breccia-sealings show diverse mineralogy and vary in colour and appearance from one sample to the other. No cross-cutting relation between breccia-fillings and calcite-fluorite has been identified but the breccia-fillings are thought to be the older of the two fillings based on the mineralogy.

## 7.1 Breccia-fillings

The breccia-fillings are dominantly made up of albite, muscovite, quartz and Fe-rich chlorite, and subordinately of hematite, fluorite, illite and K-feldspar. Illite may be precipitated at lower temperature than the breccia-fillings. Angular fragments from the wall rock are incorporated into the breccia. The fillings are commonly a couple of millimetres thick and vary in colour from greenish to reddish brown, depending on chlorite and hematite contents, respectively. Occasionally the breccia-fillings are a couple of centimetres in width (cf KKR3: 651.75–651.79 m)

The specific mineralogy of these breccia-fillings is not recognised in fracture fillings in the adjacent TIB rocks. Early formed fillings in the TIB-rocks are usually rich in epidote, quartz, chlorite, and subsequent prehnite /Drake and Tullborg 2004, 2005/. The mylonites in the TIB-rocks are usually dominated by epidote and quartz but muscovite has also been identified /Drake and Tullborg 2005/. It appears as the first formed fracture filling events in the TIB-rocks initially are dominated by Ca-rich minerals, chlorite, quartz and subordinately albite, titanite and K-feldspar, while the earliest formed fracture-fillings in the Götemar are dominated by albite, muscovite, quartz and Fe-rich chlorite, and subordinately of hematite, fluorite, illite and K-feldspar. The TIB-rocks are initially deformed in a semi-ductile to brittle manner, with associated breakdown of plagioclase and biotite resulting in epidote, chlorite and prehnite fillings in fractures. The Götemar granite is initially deformed in a brittle manner and generally lack signs semi-ductile deformation. The TIB-rocks have a

much higher Ca-content than the Götemar granite. This is also reflected by the breccia sealing minerals which indicate precipitating from locally derived fluids. Therefore the early fracture mineralogy in the Götemar granite is difficult to relate the fracture filling generations in the TIB-rocks. For example, no epidote, prehnite or laumontite (possibly only one small crystal), which are common as fracture fillings in TIB-rocks /Drake and Tullborg 2004, 2005, 2006a/ have been identified in fractures in the Götemar granite.

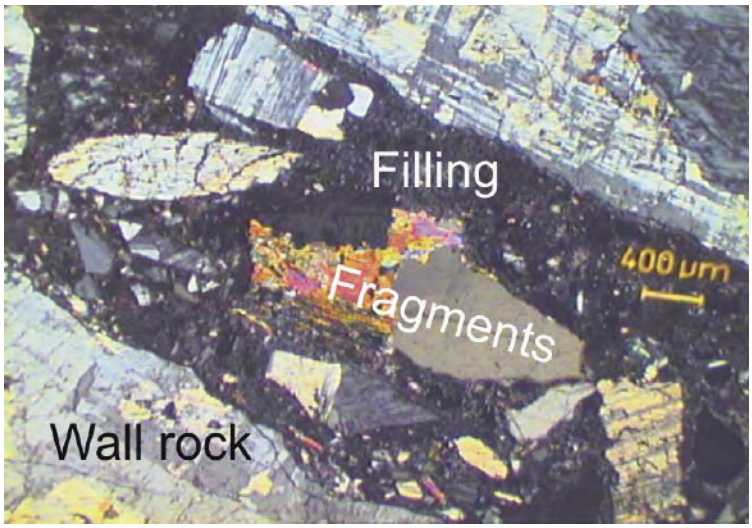


***Figure 7-1.*** *Microphotograph of a fine-grained breccia- filling and more coarse-grained fragments of the wall rock. Sample KKR1: 492.75–492.80 m.*

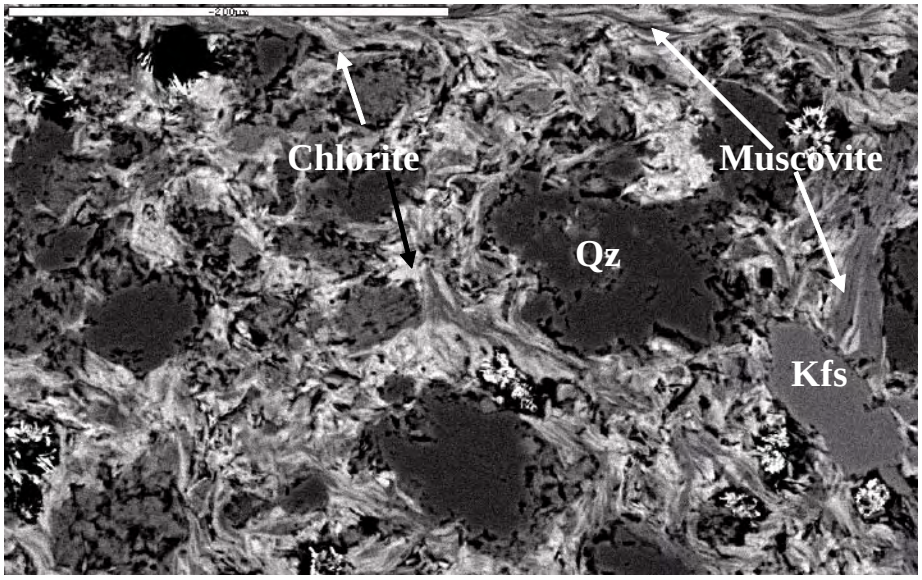


***Figure 7-2.*** *Back-scattered SEM-image of a fine-grained breccia-filling with more coarse-grained fragments of quartz (Qz) and K-feldspar (Kfs).The breccia-filling consists of Fe-rich chlorite (bright fine-grained minerals) and muscovite (darker fine-grained minerals). Scale marker bar is 200 µm. Sample KKR3: 733.55–733.58 m.*

## 7.2 Calcite-fluorite-rich fillings

Common fracture fillings in the Götemar granite are calcite, fluorite, quartz, chlorite, pyrite and subordinately galena, hematite, sphalerite, barite, U-silicate, REE-carbonate, Cu-oxide, adularia, apatite, chalcopyrite and wolframite. Formation of fluorite has been dated to 405 ± 27 Ma /Sundblad et al. 2004/. The sampled fractures are sometimes sealed, sometimes partly sealed with voids of freely growing crystals and sometimes open, with euhedral crystals covering the fracture surface. The fluorite crystals are cubic and the calcite crystals are commonly elongated along the c-axis with scalenohedral morphology. Fluorite is commonly present close to the wall rock and calcite is usually found in the middle of the sealed fractures (Figure 7-3), and on top of fluorite crystals in open fractures. Investigations of fracture surfaces show that these minerals are paragenetic. The fractures are commonly less than a centimetre wide and wider than in the calcite filled fractures in the TIB-rocks.

Platy chlorite crystals are sometimes present as a dark green cover on the fracture surfaces along with euhedral fluorite, quartz and calcite crystals (Figure 7-4). Chlorite is also found as a light green cover on cubic fluorite crystals on some fracture surfaces (Figure 7-5a). The chlorite is Fe-rich and occurs together with mixed-layer clay of presumed corrensite type. No detailed investigations of the clay mineral content have however been carried out.

Cubic pyrite cubic crystals are present, preferably on euhedral fluorite and calcite crystals on fracture surfaces (Figure 7-5), but are occasionally found within calcite crystals.

Similar fillings of scalenohedral calcite and cubic fluorite have been reported from Simpevarp, Äspö and Laxemar e.g. /Drake and Tullborg 2004, 2005, 2006a/. These fracture fillings are often present in open fractures or in very thin, sealed fractures, occasionally in association with adularia, apophyllite, barite, harmotome, REE-carbonate, corrensite, pyrite, Fe-rich chlorite, U-silicate, Cu-oxide, gypsum, sylvite, sphalerite, galena, chalcopyrite, Ti-oxide, illite, laumontite, wolframite and quartz and are presumed to be formed late in the fracture filling sequence of the TIB-rocks of the area /Drake and Tullborg 2004, 2005, 2006a/. The mineralogy of these TIB-fillings seems to be closely related to the Götemar fillings described here. Fluid inclusion data from calcite and fluorite from the Götemar granite give homogenisation temperatures of about 80–160°C (100–150°C) and salinity of about 16–23 eq. wt. % $CaCl_2$-NaCl /Alm and Sundblad 2002/. This is in agreement with fluid inclusion data from scalenohedral calcite from the TIB-fillings showing homogenisation temperatures of about 57.5–122°C (no monophase) and salinity of about 16–20 eq. wt. % $CaCl_2$ /Milodowski et al. 2005/.

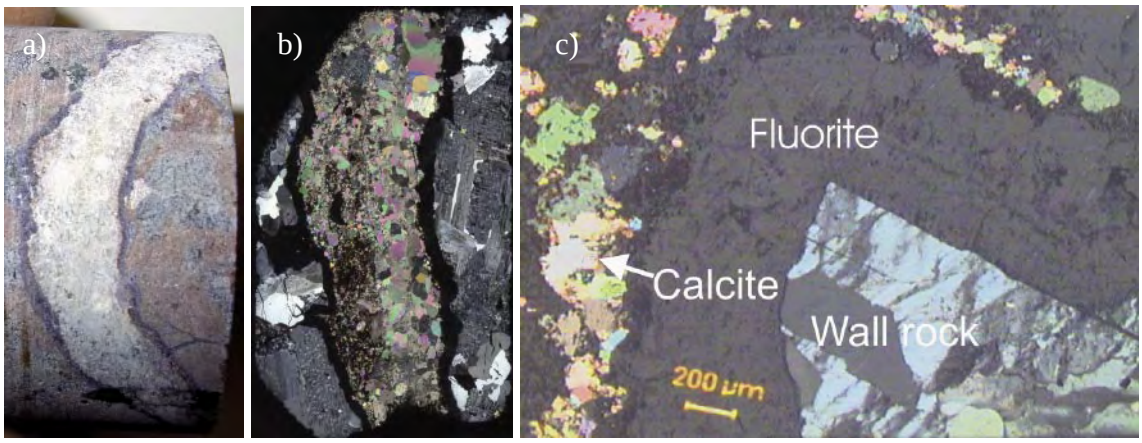


***Figure 7-3 (a–c).*** *Photograph (a), scanned thin section (b, +nic) and microphotograph (c) of a sealed fracture filled with fluorite and calcite. Typically, fluorite grows closest to the wall rock in most of the sampled calcite-fluorite bearing fractures. Sample KKR3: 52.25–52.37 m.*

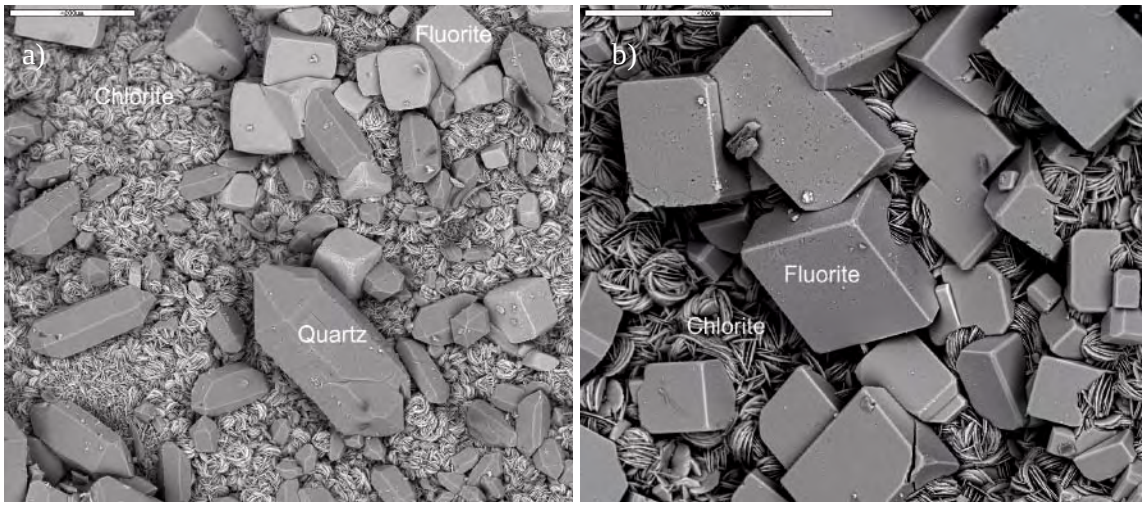


***Figure 7-4 (a–b).*** *Back-scattered SEM-images of cubic fluorite crystals, darker quartz crystals (only present in "a") and platy, more fine-grained chlorite crystals. Scale bars are 200 µm. Sample KKR2: 367.58–367.73m (a) and sample KKR2: 258.24–258.41 m (b).*

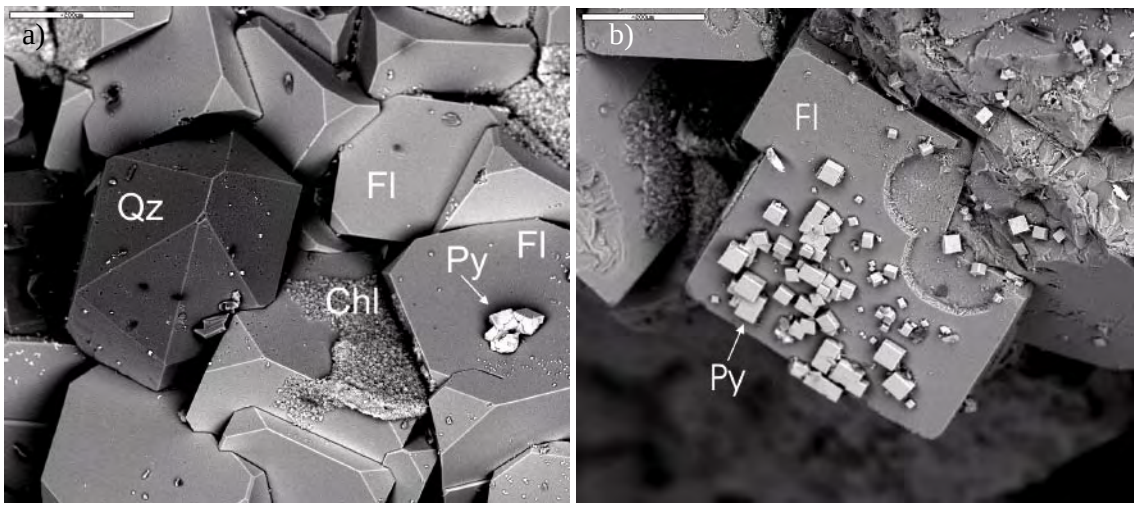


***Figure 7-5 (a–b).*** *Back-scattered SEM-images of euhedral fluorite (Fl) and quartz (Qz only in "a") with cubic crystals of pyrite (Py) and a thin cover of chlorite (Chl) on the crystal surfaces. Scale bars are 200 µm. Sample KKR3: 54.83–54.86 m (b) and sample KKR3: 539.04–539.12 m (a).*

Fluorite that penetrates fractures filled with sandstone of presumed Cambrian age is described below in accordance with /Kresten and Chyssler 1976, Alm and Sundblad 2002/.

Comparisons of SEM-EDS analyses of chlorite from Götemar fracture-fillings and from Simpevarp, Laxemar and Äspö show that chlorite in the Götemar breccia-sealings does not correlate very well with chlorite from the other sites, although some similarities with the Fe-rich chlorite exist (Figures 7-6 and 7-7). However, the chlorite that is found in relation with calcite and fluorite in the Götemar granite ("Götemar-late" in Figures 7-6 and 7-7) shows good chemical-correlation to Fe-rich chlorite from the calcite-fluorite generation in the TIB-rocks which further supports that these generations are correlated.

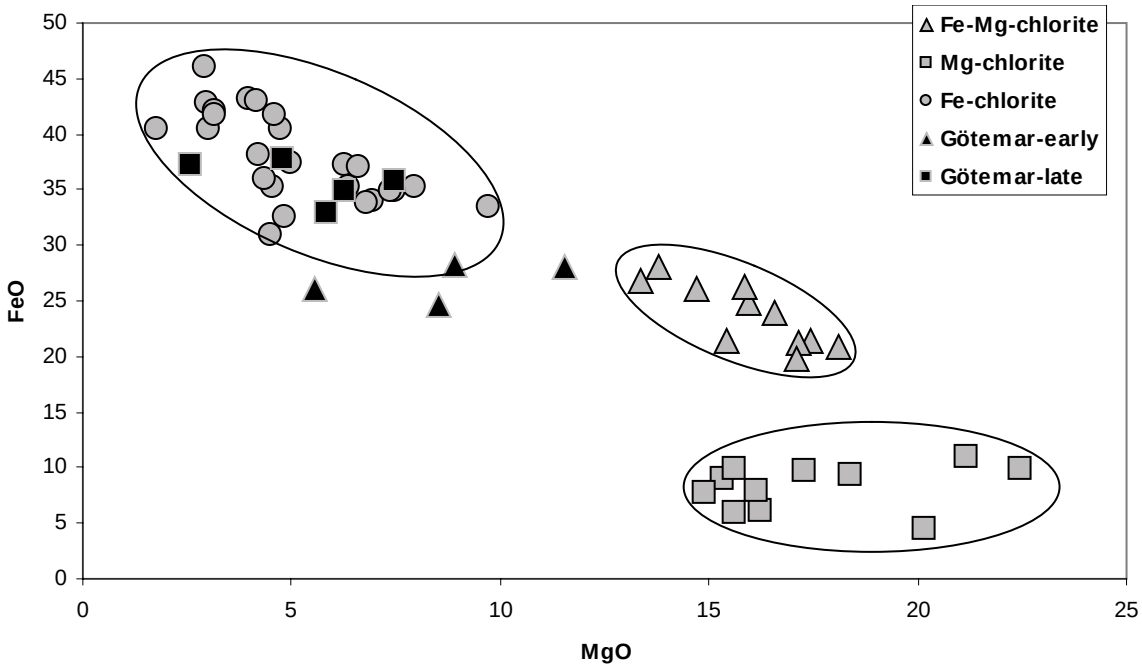


***Figure 7-6.*** *Plot of FeO vs. MgO of SEM-EDS analyses of chlorite from Götemar fracture fillings compared to fracture fillings (Fe-Mg-chlorite, Mg-chlorite, Fe-chlorite) from Simpevarp, Laxemar and Äspö /Drake and Tullborg 2004, 2005, 2006a/.*

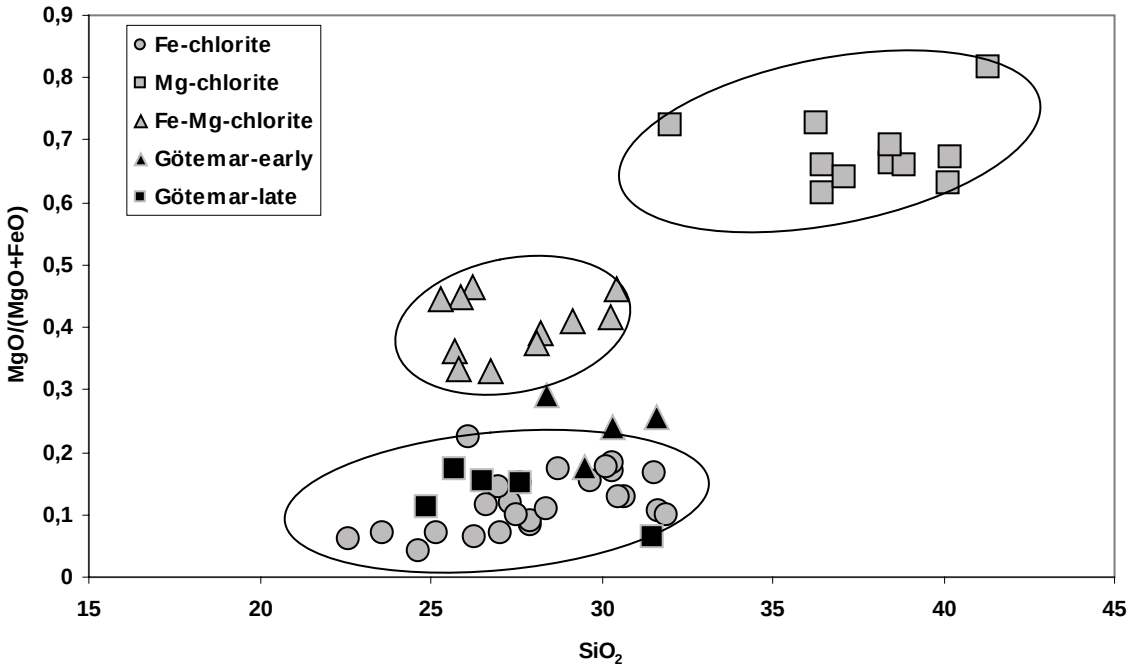


***Figure 7-7.*** *Plot of MgO/(MgO+FeO) vs. $SiO_2$ of SEM-EDS analyses of chlorite from Götemar fracture fillings compared to fracture fillings (Fe-Mg-chlorite, Mg-chlorite, Fe-chlorite) from Simpevarp, Laxemar and Äspö /Drake and Tullborg 2004, 2005, 2006a/.*

The fluorite in this paragenesis is most probably dissolved and mobilised from the wall rocks. The large amounts of Ca introduced to the fracture system in connection to this generation can hardly be explained by leaching of the Ca-poor Götemar granite (cf Section 3.1). Instead, calcium must have emanated from other sources, possibly from overlying sediments like Ordovician limestone that is now eroded, but still present in the Baltic Sea and on Öland nearby. Thick overlying sediments could also have been responsible for the elevated fluid temperatures that induced precipitation of these fillings in the fractures. Such sediments have most probably included sequences of Silurian to Devonian sediments reported to have covered large parts of Sweden /Bassett 1985, Zeck et al. 1988, Tullborg et al. 1996, Larson et al. 1999a, Larson et al. 1999b, Cederbom et al. 2000/. A majority of the calcite-fluorite bearing fractures described by /Alm and Sundblad 2002/ strike NE-SW and have sub-vertical dips, which might indicate a regional compression in this direction or an extension in NW-SE, possibly related to a SE-migrating Caledonian foreland basin /Alm et al. 2005/.

## 7.3 Sandstone

Thin sections of two fractures filled with alleged Cambrian sandstone from Kråkemåla quarry #2 have been investigated in this study. The sandstone is about one centimetre thick in both samples. Fluorite-bearing fractures, with small amount of calcite, are present along both of the sandstone-wall rock (granite) contacts. Pale violet fluorite has also entered into the sandstone as fine-grained cement, occasionally made up of larger euhedral crystals. The cement also contains smaller amounts of fine-grained quartz and K-feldspar. The sandstone is made up of rounded clasts of quartz and subordinate, angular feldspar crystals (Figure 7-8a). The quartz crystals show partly dissolution textures along the grain-boundaries and the feldspar crystals show signs of dissolution, which indicates that the grains have been in contact with reactive fluids (Figure 7-8b). No major grain-size differences or trends in the amount of fragments exist within the sandstone veins. However, in one sample the middle of the vein contains more fine-grained clasts than along the contact to the fluorite filling. In the other sample more fine-grained clasts can be found close to one of the sandstone-fluorite filling contacts.

The thin section investigation indicates that initially, the very porous sandstone might have been consolidated by precipitation of quartz. Fluorite was probably not the primary cement and it entered the porous sandstone through F-rich fluids in fractures along the contacts to the wall rock and filled the pore space in the sandstone and might have dissolved parts of some of the quartz crystals. The fact that quartz fragments from the sandstone are present in the adjacent fluorite filling, with a higher amount of fragments close to the sandstone-fluorite filling contact (Figure 7-9), further indicates that fluorite entered the sandstone subsequently to consolidation. This is all in agreements with detailed observations by /Alm and Sundblad 2002/.

The relation between the calcite-fluorite fillings and Cambrian sandstone dykes is a clear indication of a Cambrian maximum age for the calcite-fluorite fillings. This is also in agreement with earlier work in the region /Kresten and Chyssler 1976, Alm and Sundblad 2002, Röshoff and Cosgrove 2002, Sundblad et al. 2004, Alm et al. 2005/.

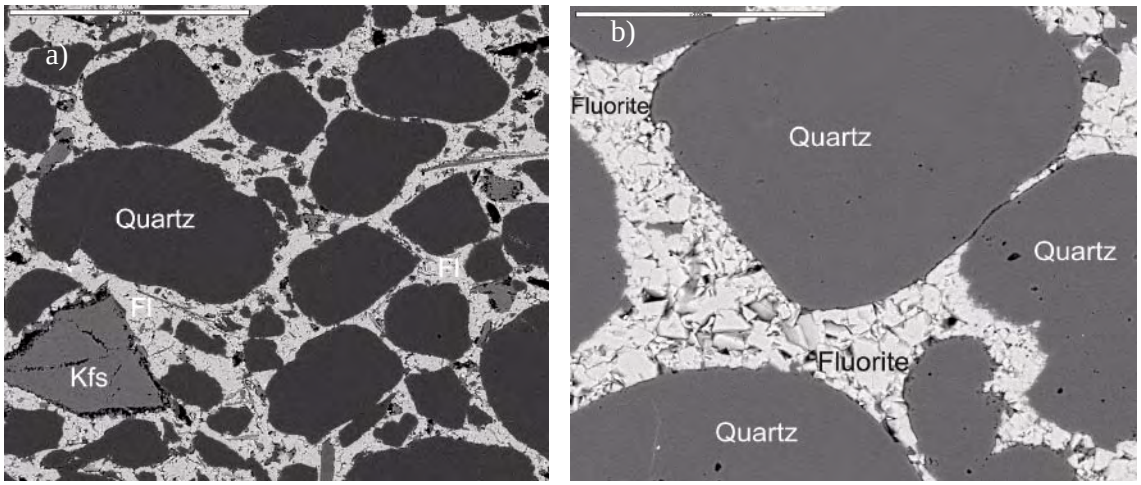


***Figure 7-8 (a–b).*** *Back-scattered SEM-image of sandstone made up of fluorite cement and mostly rounded quartz clasts and angular K-feldspar clasts (Kfs). Quartz clasts are partly dissolved (b) and euhedral fluorite can be found in the cement (b). Scale bar is 200 µm.*

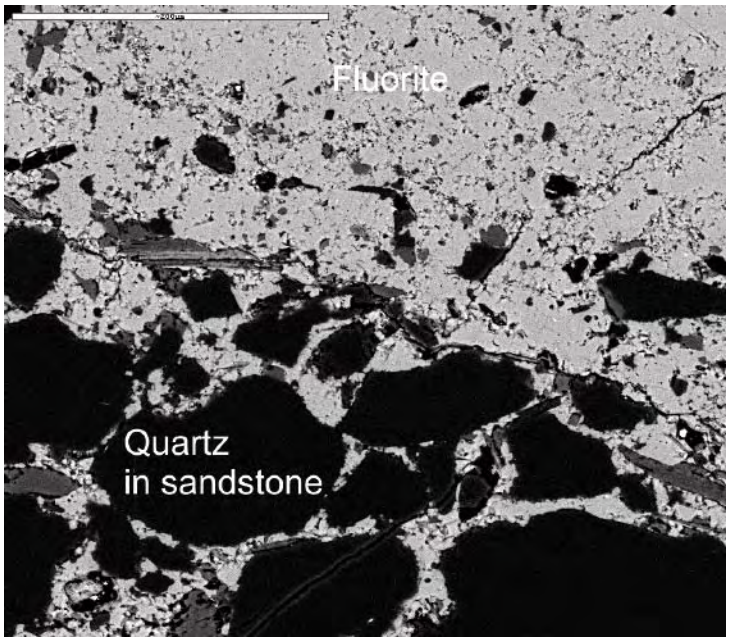


***Figure 7-9.*** *Back-scattered SEM-image of the contact zone between sandstone and the fluorite-filling. Fragments of quartz and K-feldspar form the sandstone is found within the fluorite-filling, mostly close to the contact. Scale bar is 200 µm.*

## 7.4 Stable isotopes

Results and interpretations of stable isotope analyses of $\delta^{18}O$, $\delta^{13}C$ and $^{87}Sr/^{86}Sr$ in calcite, $^{87}Sr/^{86}Sr$ in fluorite and $\delta^{34}S$ in pyrite from fracture fillings are presented in this section. Results of the stable isotope analyses are found in Table 7-1.

**Table 7-1. Isotope analyses of calcite ($\delta^{13}C$, $\delta^{18}O$, $^{87}Sr/^{86}Sr$), fluorite ($^{87}Sr/^{86}Sr$) and pyrite ($\delta^{34}S$).**

| Sample | $\delta^{13}C$ (‰ PDB) | ± | $\delta^{18}O$ (‰ PDB) | ± | $^{87}Sr/^{86}Sr$ calcite | ± | $^{87}Sr/^{86}Sr$ fluorite | ± | $\delta^{34}S$ (‰ CDT) |
|---|---|---|---|---|---|---|---|---|---|
| KKR02: 23.12–23.25 | –12.090 | 0.1 | –10.457 | 0.1 | | | | | |
| KKR02: 48.95–49.00(I) | –47.091 | 0.1 | –8.046 | 0.1 | 0.717257 | 0.000045 | | | |
| KKR02: 48.95–49.00(II) | –44.825 | 0.1 | –8.328 | 0.1 | | | | | |
| KKR02: 171.52–171.61 | –16.316 | 0.1 | –7.893 | 0.1 | | | | | |
| KKR02: 213.42–213.55 | –23.243 | 0.1 | –10.365 | 0.1 | | | | | 58.3 and 60.8* |
| KKR02: 213.90–214.00 | –16.286 | 0.1 | –7.068 | 0.1 | 0.717166 | 0.000016 | 1.409888 | 0.000041 | 46.6 |
| KKR02: 236.69–236.84 | –15.153 | 0.1 | –13.692 | 0.1 | 0.716950 | 0.000016 | 1.187298 | 0.000032 | |
| KKR03: 52.25–52.37 | –11.137 | 0.1 | –14.263 | 0.1 | 0.715983 | 0.000014 | 0.794862 | 0.000012 | |
| KKR03: 54.83–54.86(I) | –11.661 | 0.1 | –13.599 | 0.1 | | | | | |
| KKR03: 54.83–54.86(II) | –12.632 | 0.1 | –12.766 | 0.1 | | | 0.715806 | 0.000013 | 13.2 |
| KKR03: 75.20–75.30 | –11.831 | 0.1 | –14.911 | 0.1 | | | 0.731849 | 0.000117 | 17 |
| KKR03: 389.11–389.13 | –6.444 | 0.1 | –8.695 | 0.1 | | | | | |
| KKR03: 459.02–459.12 | –13.169 | 0.1 | –14.142 | 0.1 | | | | | |
| KKR03: 539.04–539.12 | –10.425 | 0.1 | –14.538 | 0.1 | 0.716590 | 0.000017 | | | |

* The analyses were performed on material from the same bulk sample, divided into two parts.

### 7.4.1 Fracture calcite

In order to distinguish different generations and to provide possible palaeohydrogeological information 12 samples (of which two samples were analysed twice) have been analysed for $\delta^{13}C$ and $\delta^{18}O$, of which five samples have been selected for $^{87}Sr/^{86}Sr$ analyses (Table 7-1). The calcites represent both sealed and open fractures. In some open fractures it has been possible to sample calcites with euhedral, often scalenohedral crystal forms (elongated c-axis). The $\delta^{13}C$ and $\delta^{18}O$ values for the Götemar calcites are plotted together with previously analysed calcites from Simpevarp and Laxemar (Figure 7-10). The Götemar calcites show $\delta^{18}O$ values ranging from about –14.5 to –7.1‰ (PDB) and $\delta^{13}C$ values from –47.1 to –6.4‰ (PDB).

Five calcites (one of these samples was analysed twice) show $\delta^{18}O$ values between –14.5 and –12.8‰ and $\delta^{13}C$ values between –15.1 and –10.4‰, which is in agreement with isotope ratios recorded in calcites with scalenohedral shape, identified at Äspö, Simpevarp and Laxemar /Bath et al. 2000, Drake and Tullborg 2004, Tullborg 2004, Drake and Tullborg 2006a/. The scalenohedral shape is interpreted as saline fluid precipitates which is also supported by the very high salinities measured in fluid inclusions from this type of calcite /Milodowski et al. 2005/. Therefore this group of calcites is indicated as possible “warm brine“-precipitates. These five scalenohedral calcites from Götemar are generally in paragenesis with e.g. fluorite, pyrite, galena, barite, sphalerite and REE-carbonate. The samples are from sealed, partially sealed and open fractures.

Four calcite samples show $\delta^{18}O$ values between –10.5 and –7.9‰ and large variation in their $\delta^{13}C$ carbon isotope values (–6.4 to –47.1‰). This supports interaction with biogenic carbon to various degrees. The extreme $\delta^{13}C$ value (–47.1‰) suggests biogenic activity in the groundwater aquifers causing disequilibria in situ. It should be noted that the fractionation between $HCO_3^-$ and $CaCO_3$ is only a few per mille and the $\delta^{13}C$ value in the calcite therefore largely reflects the $\delta^{13}C$ value in the bicarbonate at the time of calcite formation. In situ activity of microbes indicates largely temperatures below 100°C and a low temperature origin for these calcites is thus suggested. If assuming formation temperatures as low as the ambient 7–15 °C, the calcites may have formed from water similar to the present meteoric or brackish Baltic Sea water at site (based on fractionation factors by /O’Neil et al. 1969/).

Two of these four additional samples ($\delta^{13}C$: –12.1 and –16.3‰; $\delta^{18}O$ –10.5 and –7.9‰) consist of thin calcite layers from open fractures, clearly different from the calcite-fluorite fillings. Another sample (KKR02: 48.95–49.00 m analysed twice; $\delta^{13}C$ = –47.1 and –44.82‰; $\delta^{18}O$ = –8.0 and –8.3‰, respectively) is from a characteristic calcite-fluorite filling. This differs considerably in isotopic composition from the other calcite-fluorite samples which might reflect that some scalenohedral calcites show strong $\delta^{13}C$-fractionation or that overgrowth of younger calcite is included in the isotope analysis. Some scalenohedral calcites in paragenesis with pyrite, barite, apophyllite etc from Laxemar also show these extremely low $\delta^{13}C$-values /Drake and Tullborg, in manuscript/. Two of the Götemar samples ($\delta^{13}C$: –23 and –10‰; $\delta^{18}O$ = –16 and –7‰, respectively) show values in between the scalenohedral calcites precipitated from warm brine waters and the calcites precipitated from more meteoric to brackish waters. These samples might include a mixture of calcites with at least two different isotope signatures (origins). However, it is for the moment not possible to conclude if these calcites are late stage (low temperature) precipitates within calcite-fluorite generation or are precipitated much later in time (possibly Quaternary).

In studies of Laxemar, Äspö and Simpevarp, calcites showing very low $\delta^{18}O$ values (about –23 to –15‰) and $\delta^{13}C$ values between about –2 and –6‰, typical for hydrothermal calcites without signs of biogenic carbon, were found (Figure 7-10). This type of calcite has not been found in the Götemar granite.

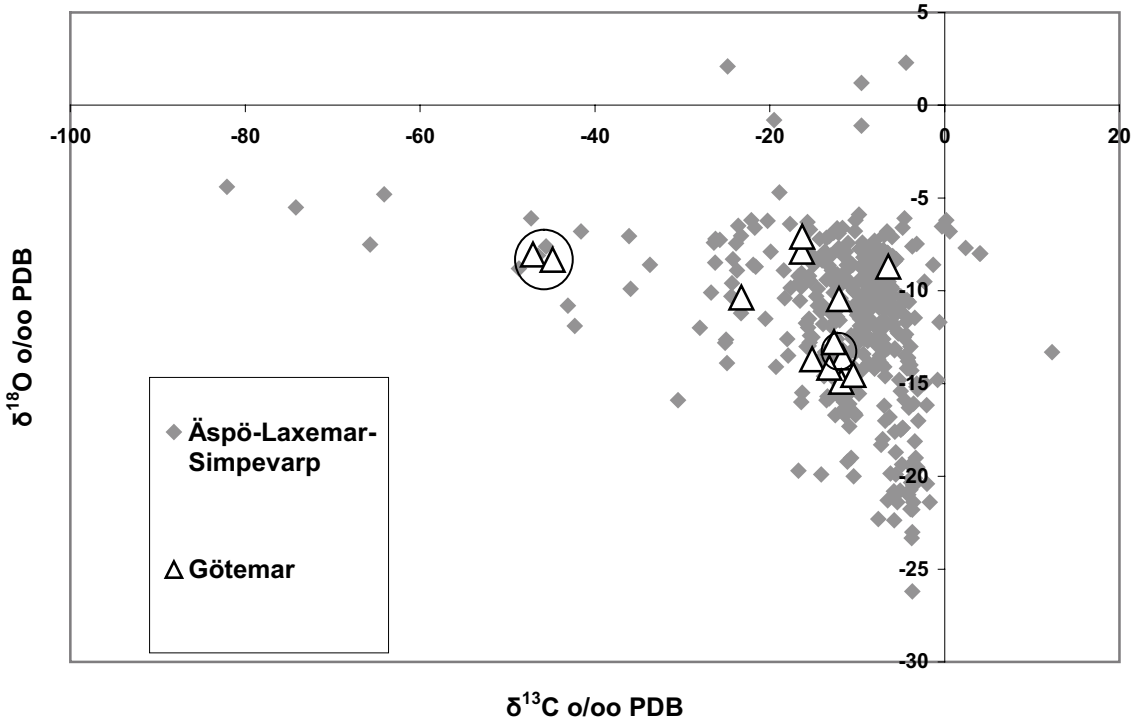


***Figure 7-10.*** *$\delta^{13}C/\delta^{18}O$ values for fracture calcites in Götemar plotted together with earlier analysed samples from Äspö/Laxemar /Tullborg 1997, Wallin and Peterman 1999, Bath et al. 2000/, KSH01, Simpevarp /Drake and Tullborg 2004/, KSH03 /Drake and Tullborg 2006a/, Simpevarp, KLX03, KLX04, KLX05 and KLX06, Laxemar /Drake and Tullborg, in manuscript/, KA1755A and KAS17 Äspö /Drake and Tullborg, unpublished data/. Values within the circles are from the same sample.*

The Sr isotope values in the five analysed fracture calcites range from about 0.716 to 0.717. A plot of Sr-isotope ratio versus $\delta^{18}O$ values for fracture calcites in Götemar and KSH01 /Drake and Tullborg 2004/ and KSH03 /Drake and Tullborg 2006a/, KLX03, KLX04, KLX05 and KLX06 /Drake and Tullborg, in manuscript/ and KA1755A and KAS17 /Drake and Tullborg, unpublished data/ is shown in Figure 7-11.

There is a general trend of higher $^{87}Sr/^{86}Sr$ ratios in samples with higher $\delta^{18}O$ values which is in agreement with earlier observations by /Wallin and Peterman 1999, Bath et al. 2000, Drake and Tullborg 2004, 2006a/, showing the lowest $^{87}Sr/^{86}Sr$ isotope ratios and the lowest $\delta^{18}O$ values for the hydrothermal calcites. The analysed calcites from the Götemar granite show relatively high $^{87}Sr/^{86}Sr$ isotope ratios compared to the TIB calcites with the same $\delta^{18}O$ values /Drake and Tullborg 2004, 2006a/. However, the paragenesis and the $\delta^{13}C$- and $\delta^{18}O$-values suggest that the calcites from fractures in the Götemar granite and the Laxemar and Simpevarp subareas are precipitated during similar conditions. The higher $^{87}Sr/^{86}Sr$ ratios in the Götemar granite calcites may be due to enhanced addition of radiogenic Sr from the K (and Rb) rich Götemar granite. This scenario is also supported by the fact that calcite samples from Simpevarp generally show lower $^{87}Sr/^{86}Sr$ ratios than the Laxemar calcites, which may be due to a lower K (and Rb) content in Simpevarp since the bedrock at Simpevarp is dominated by rocks of quartz monzodioritic composition while the Laxemar subarea is dominated by Ävrö granite. /Drake and Tullborg, in manuscript/.

Sr isotope values for groundwater at Simpevarp are presently about 0.715 to 0.716 /Laaksoharju et al. 2004/. This suggests that some of the calcite from Simpevarp of this generation has precipitated from fluids with similar Sr-ratios as the present groundwater. Unfortunately no values are available from groundwater in the Götemar granite.

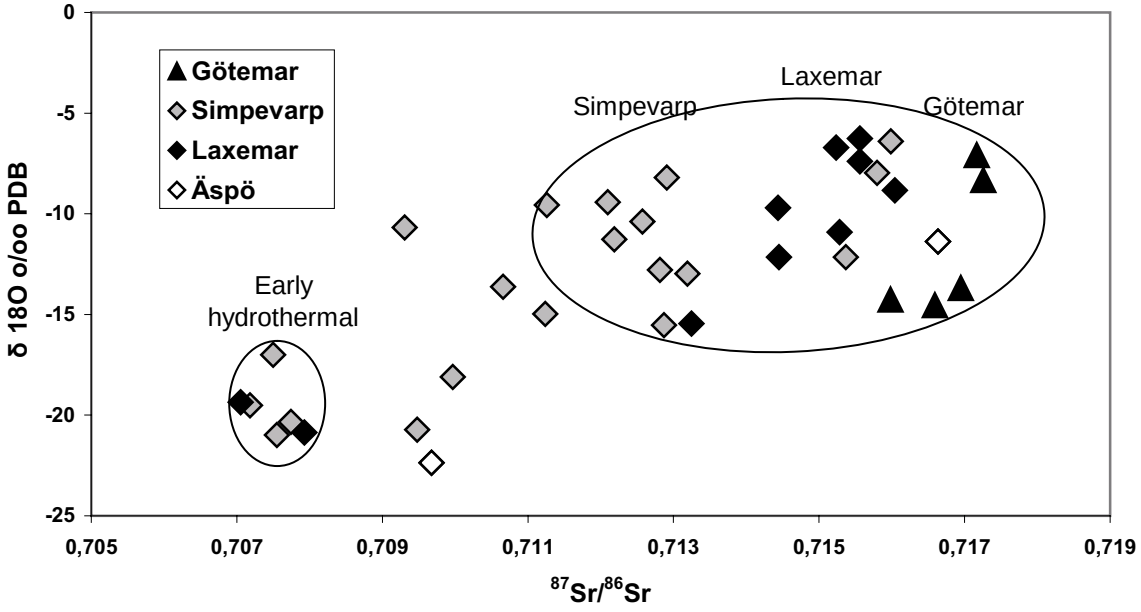


***Figure 7-11.*** *Sr isotope ratio plotted versus $\delta^{18}O$ values for fracture calcites in Götemar and KSH01 /Drake and Tullborg 2004/, KSH03 /Drake and Tullborg 2006a/, KLX03, KLX04, KLX05,KLX06 /Drake and Tullborg, in manuscript/, KA1755A and KAS17 /Drake and Tullborg, unpublished data/. Encircled samples to the left show early hydrothermal calcites and encircled samples to the right show dominantly scalenohedral calcite having similar paragenesis and $\delta^{13}C$/ $\delta^{18}O$-ratios.*

### 7.4.2 $^{87}Sr/^{86}Sr$ in fluorite

Five fluorite samples have been analysed for $^{87}Sr/^{86}Sr$ (Table 7-1). Only one of the five samples (KKR03: 54.83–54.86) has a Sr-ratio (0.716) in correspondence with the Sr-ratios of calcite from the same fracture filling paragenesis (0.716 to 0.717). The other samples show elevated, sometimes extreme, $^{87}Sr/^{86}Sr$-ratios. Fluorite is always present next to the fracture wall and calcite has filled the assumed newly formed fractures subsequently. Since the Götemar granite is rich in K and Rb, the initial fluids in the fractures have probably been highly enriched in $^{87}Sr$ from decay of $^{87}Rb$ in the wall rock minerals (muscovite, K-feldspar and biotite). An explanation for the elevated $^{87}Sr$ values in most of the fluorite samples compared to the calcite could be that the fluorite is formed from a fluid that locally was enriched in radiogenic $^{87}Sr$ due to selective leaching of e.g. muscovite in the fractures and that the calcite precipitated later when the $^{87}Sr/^{86}Sr$-ratio was more homogenized,. Another possibility is that the analysed samples contain small amounts of K-bearing minerals from the wall rock, resulting in enriched $^{87}Sr/^{86}Sr$-ratios.

### 7.4.3 $\delta^{34}S$ in pyrite

#### *Short review*

Sulphur has four stable isotopes, of which the ratio of $^{34}S$ and $^{32}S$, expressed as $\delta^{34}S$ per mil (‰) by relating the measured $^{34}S/^{32}S$ to a reference standard (CDT), is used for interpretation of S-isotope variations. The CDT-standard comes from troilite of the Canyon Diablo iron meteorite. The $^{34}S/^{32}S$-ratio in both sedimentary and igneous environments can change with many variables like pH of solutions, nature of the ions, oxygen fugacity, temperature, reaction rates etc, although the greatest fractionation of the sulphur isotopes occur during oxidation-reduction reactions /Ohmoto 1972, Krauskopf and Bird 1995 and references

therein/. Two general types of fractionation mechanisms are responsible for the naturally occurring sulphur isotope variations; 1) kinetic isotope effects during microbial processes and 2) various inorganic chemical exchange reactions between sulphides/sulphates and between different sulphides /Hoefs 2004 and references therein/.

A large group of organisms gain energy by reducing sulphate while oxidizing organic carbon, preferentially in anoxic environments. These organisms can tolerate temperatures up to about 100°C or slightly higher (up to 120°C) and salinities from fresh water to brines /Jorgensen et al. 1992, Machel et al. 1995, Canfield 2001/. Sulphate reducing bacteria normally produce $^{34}S$-depleted sulphide e.g. /Harrison and Thode 1957, Chambers et al. 1976/. In a "closed" system with a limited reservoir of sulphate, preferential loss of the lighter isotope from the reservoir influence the isotopic composition of the unreacted source material in that the $^{34}S$-composition of residual sulphate steadily increase with sulphate consumption (Rayleigh distillation) e.g. /Ohmoto and Goldhaber 1997/. The derived sulphide may thus become heavier than the original sulphate when about $^{2}/_{3}$ of the reservoir has been consumed. These reactions during gradually changed conditions may produce sulphides whose isotopic composition varies strongly with time, sometimes visible as zoned crystals (light cores and heavier rims) or heterogeneous sulphur isotope ratios in the same vein or fracture /McKibben and Eldridge 1994/.

Abiotic thermochemical sulphate reduction reduces sulphate to sulphide under the influence of heat rather than bacteria, although the question of whether this reduction can take place at temperatures as low as about 100°C, in the ranges of the upper limit of microbiological reduction is debated /Trudinger et al. 1985/. /Ohmoto and Goldhaber 1997/ argued that thermochemical reduction is not effective at temperatures below 125°C because of slow reaction kinetics, although it has been observed at much lower temperatures (≈ 80°C) e.g. /Orr 1974/. It is often suggested that S-isotope fractionations are small during thermochemical reduction /Orr 1974/ although there exist indications of S-isotope fractionations of 10 to 20‰ at temperatures of 100–200°C /Kiyosu and Krouse 1990/. Partial oxidation of a sulphide mineral to a sulphate mineral results in an enrichment of $^{34}S$ over $^{32}S$ in the sulphate /Brownlow 1996 and references therein/. Sulphides from igneous rocks show a narrow range of $\delta^{34}S$-values (–3 to +3‰), /Ohmoto and Rye 1979, Field and Fifarek 1985/) while sedimentary sulphides (+42 to –45) and sulphides from ore deposits (+50 to –45 in sedimentary rocks and +7 to –7 in igneous rocks) show wide variations in isotopic composition cf /Brownlow 1996, Hoefs 2004 and references therein/.

In sedimentary rocks, highly enriched $\delta^{34}S$ values in pyrite have been explained as the result of progressive pyrite crystallization in a sulphate-limited "closed" system e.g. /McKay and Longstaffe 2003/. Such conditions are expected in marine sediments as burial occurs, and in brackish, low sulphate sediments such as coastal plains. Rapid burial in marine environments below the depth where sulphate is added to the sediment from the overlying seawater leads to crystallization of pyrite with high $\delta^{34}S$ values e.g. /McKay and Longstaffe 2003 and references therein/. $\delta^{34}S$ values of up to +67‰ have been measured for sulphides from freshwater sedimentary units e.g. /Cole and Picard 1981/.

### *Results*

Euhedral pyrite from four open fractures have been analysed for $\delta^{34}S$. The sampled pyrite crystals are interpreted on textural grounds to have been formed in association with the wide-spread calcite-fluorite precipitation in fractures, which in turn has been formed at temperatures of about 80–160°C based on fluid inclusion studies on fluorite and calcite /Alm and Sundblad 2002/ at 405 ± 27 Ma /Sundblad et al. 2004/.

The analyses yielded $\delta^{34}S$-results of 13.2 to 60.3‰ for samples from 54 to 214 m depth (Figure 7-12). The two highest values for the Götemar samples are considerably higher in $^{34}S$ than from presumed contemporaneous pyrite crystals from Simpevarp and from Laxemar (Figure 7-12) /Drake and Tullborg, in manuscript/. However, the two lowest results from the Götemar samples are similar to that of pyrite in similar paragenesis from Simpevarp and Laxemar (Figure 7-12).

The $\delta^{34}S$-composition of the Kråkemåla (KKR02 and KKR03) pyrites is clearly different from the composition of older pyrite crystals (Figure 7-12) from Simpevarp and Laxemar (KSH01, KLX03 and KLX06). The latter have $\delta^{34}S$-values of –3 to 0.5‰ that are characteristic for pyrite formed from hydrothermal fluids at higher temperatures than the paragenesis studied cf {Ohmoto 1979 #227; /Field and Fifarek 1985/}.

The higher values of the Götemar pyrites (46.6 to 60.3‰) are too high to be explained by thermochemical fractionation. High fractionation from microbial reduction in situ, in a "closed" system, with a limited sulphate source, is a more probable process for these samples. Microbial sulphate reduction can take place at temperatures up to 100–120ºC /Jorgensen et al. 1992, Machel et al. 1995/. These temperatures overlap those determined from fluid inclusion studies /Alm and Sundblad 2002/. The elevated values in the studied

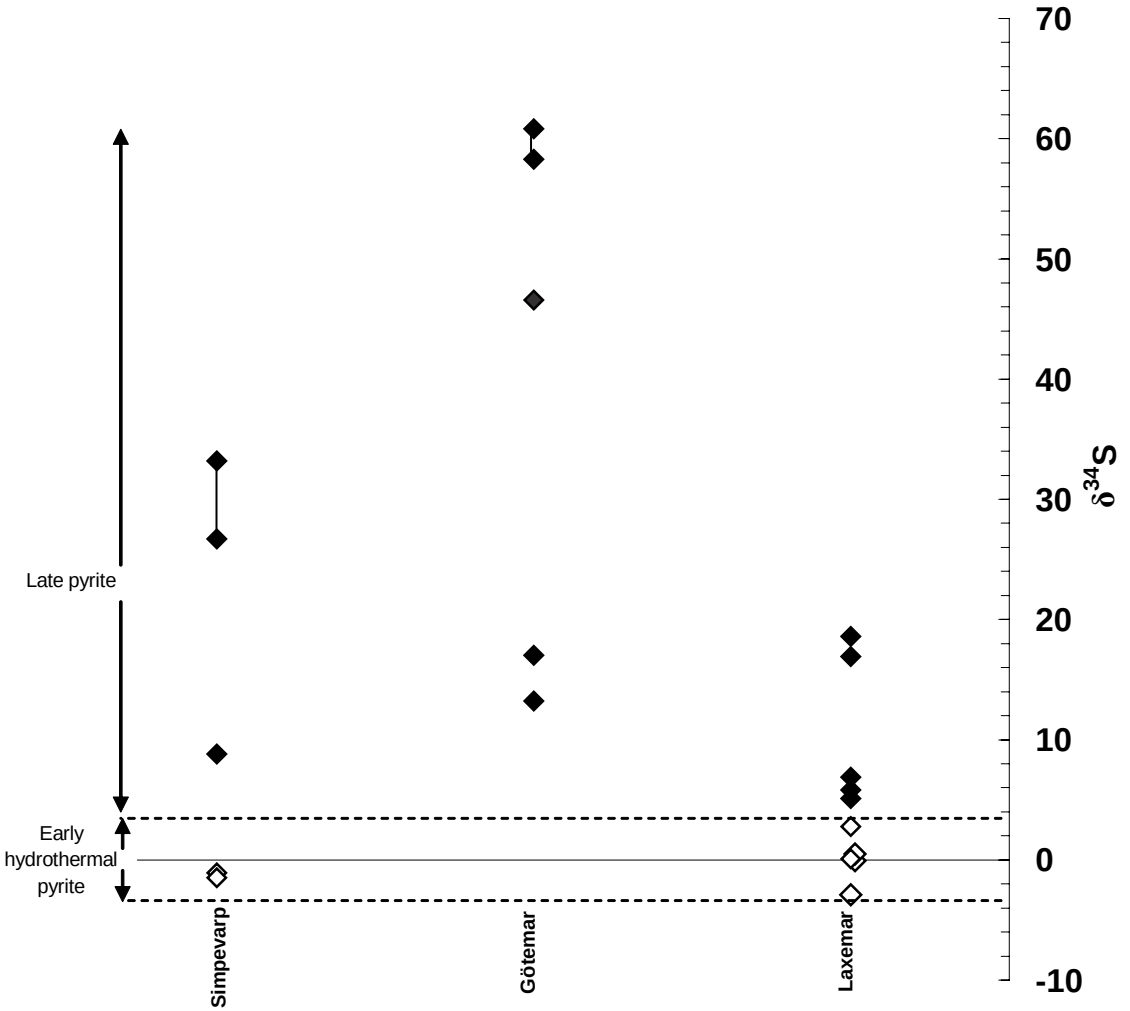


***Figure 7-12.*** *Plot of $\delta^{34}S$ value from KKR02 and KKR03 along with values from drill cores KSH01 and KSH03 from Simpevarp and KLX03, KLX04, KLX05 and KLX06 from Laxemar /Drake and Tullborg, in manuscript/. Values connected by a line are from two analyses of the same sample.*

pyrites would be a late stage product in a microbial reduction process, as a fluid undergoing a Rayleigh distillation process of in situ sulphate reduction would incorporate extremely enriched $H_2S$ in the last fraction of deposited pyrite /McKibben and Eldridge 1994/. Large local variations within the system (e.g. within the same fracture, in different fractures and at different depths) or between coeval systems may explain the large differences between the pyrite samples. The quite large spread in $\delta^{34}S$-values in two samples from Simpevarp (probably coeval with pyrite in this study) /Drake and Tullborg, in manuscript/ indicates heterogeneity which further infers fractionation in a closed system, in accordance with studies of /McKibben and Eldridge 1994/.

The moderately high values from (13.2 and 17.2‰) may have been produced by two alternative processes: 1) biogenic microbial fractionation as indicated by $\delta^{13}C$ in related calcite or, 2) non-microbial thermochemical fractionation from a sulphate rich in $^{34}S$, possibly from mixing of two fluids, perhaps at temperatures too high for microbial reduction. This would involve negligible fractionation compared to microbial fractionation /Orr 1974/, resulting in pyrite with heavy isotope values similar to its parental sulphate.

# 8 Summary

Based on the present study the Götemar granite seems to contain a smaller number of fracture filling generations than the adjacent TIB-rocks. The relative age between different fracture-filling parageneses have been difficult to establish since there exist few cross-cutting relations and re-activations of the fractures. It has however been possible to distinguish two major fracture filling generations. Based on formation conditions a relative age is proposed. Oldest is a breccia-sealing that appears in many varieties and youngest is a filling consisting of mainly, calcite, fluorite, quartz, chlorite and pyrite (see below). Stable-isotopes analyses of fracture calcites indicate that low temperature calcite crystals have precipitated in open fractures, sometimes on the surfaces of minerals of the calcite-fluorite generation. These calcite varieties might represent several events but the present set of data is too small to draw any conclusions. It is also important to mention that the drill cores from the Götemar granite were drilled with conventional technique (single barrel). Soft and small calcites grains that possibly could represent later low temperature fillings could therefore have been destroyed.

Generation 1: Breccia-sealings which dominantly consist of albite, muscovite, quartz and Fe-rich chlorite, and subordinately hematite, fluorite, K-feldspar and possibly illite. It is however somewhat unclear whether illite belongs to this generation or not. The minerals in this generation reflect the wall rock chemistry, with a high amount of K-bearing and Na-bearing fillings, and a lack of calcium-bearing minerals. No fractures in the studied Götemar granite samples contain epidote, prehnite and laumontite (possibly one observation) which are characteristic early stage minerals of the Simpevarp and Laxemar fracture fillings e.g. /Drake and Tullborg 2004, 2005, 2006a/. On the other hand, the Götemar granite is rich in K and Na but poor in Ca and breccia-filling precipitation from locally derived fluids can be suspected, which in turn implies that it is complicated to correlate the characteristic early formed fillings in these rocks. Chlorite chemistry is also slightly different for early chlorite from Götemar compared to more or less well established Simpevarp and Laxemar generations //Drake and Tullborg 2004, 2005, 2006a/. The earliest formed fracture fillings in Simpevarp and Laxemar are characterized by semi-ductile deformation, but no sign of this has been noted in the present study. This places the formation of mylonite and possibly also the major cataclasite formation in the adjacent TIB-rocks to events prior to, or possibly contemporaneous with the intrusion of the Götemar granite.

Generation 2: The calcite-fluorite fillings are presumed to be formed subsequently to the breccia-sealings, and have been dated to 405 ± 27 Ma /Sundblad et al. 2004/. These fillings also seal fractures that cross-cut sandstone of presumed Cambrian age. $\delta^{13}C$ and $\delta^{18}O$ values of calcite from this generation are similar to late formed calcite precipitated from warm brine in Simpevarp, Laxemar and Äspö /Tullborg 1997, Wallin and Peterman 1999, Bath et al. 2000, Drake and Tullborg 2004, 2006a/. One of the calcite samples from this study and some calcite samples from Simpevarp and Laxemar /Drake and Tullborg, in manuscript/ show extremely low $\delta^{13}C$ values indicating biological activity in the groundwater aquifer. The paragenesis of this calcite-fluorite generation is very similar to the young characteristic fracture filling in Simpevarp and Laxemar, although the abundance of the minerals in the paragenesis differs somewhat between the two areas. It is thus proposed that this TIB-fracture filling generation is coeval with the calcite-fluorite fracture fillings in the Götemar granite and thus formed at about 405 ± 27 Ma. This is also supported by the similarities in morphology of calcite crystals (scalenohedral) and similarities in chemistry of chlorite in the TIB-fillings and in the calcite-fluorite fillings at Götemar. The calcite-fluorite fillings are however generally more common and seal even wider fracture in the Götemar granite than in the adjacent TIB-rocks.

The $^{87}Sr/^{86}Sr$ values of the Götemar calcites are homogeneous and slightly higher than most of the $^{87}Sr/^{86}Sr$ values from Simpevarp and Laxemar calcites /Drake and Tullborg 2004, 2006a/, which may reflect different $^{87}Sr/^{86}Sr$-ratios of the wall rock. Highly enriched $\delta^{34}S$-values of pyrite and very low $\delta^{13}C$-values of calcite are occasionally observed in this generation, as well as in the related TIB-fracture fillings, and suggest some degree of biogenic activity and microbial sulphate reduction in the ground water aquifer, resulting in disequilibrium in situ. $^{87}Sr/^{86}Sr$-ratios in fluorite are generally highly enriched compared to associated calcite.

The wide-spread calcite precipitation in fractures in Götemar granite suggests that Ca is contributed to the fracture system from an external source. The calcium could be derived from adjacent TIB-rocks or Ca-rich fracture fillings in the TIB-rocks but it is not very likely, especially since the TIB-rocks apparently have lower amounts of this filling. An overlying Palaeozoic sediment cover, such as the thick Devonian sediments that evidently covered the region e.g. /Bassett 1985, Zeck et al. 1988, Tullborg et al. 1996, Larson et al. 1999a, Larson et al. 1999b, Cederbom et al. 2000/, could however provide both the increased temperature caused by burial and Ca-rich fluids necessary for the precipitation of calcite. The fractures could be induced by extension in NW-SE direction, since they dominantly strike NE-SW /Alm and Sundblad 2002/ and are possibly related to a SE-migrating Caledonian foreland basin /Alm et al. 2005/.

# 9 Acknowledgements

We would like to thank the staff at the SKB site investigations at Simpevarp for their support. Owe Gustafsson at Earth Sciences Centre, Göteborg University carried out the O and C isotope analyses on calcite. Göran Åberg at Institute for Energy Technology, Norway carried out Sr isotope analyses on calcite and fluorite. Tony Fallick at Scottish Universities Environmental Research Centre, Glasgow carried out sulphur isotope analyses on pyrite and gave support to the interpretation of the results. Kjell Helge and Ali Firoozan carried out thin section preparation. Sven Åke Larson, Göteborg University contributed with valuable comments to the manuscript. Harald Strauss, University of Münster, is thanked for comments on the sulphur isotope interpretations. Björn Sandström, Göteborg University is thanked for useful comments. Fredrik Hartz, SKB, kindly helped us with the map for the area.

# References

**Alm E, Sundblad K, 2002.** Fluorite-calcite-galena-bearing fractures in the counties of Kalmar and Blekinge, Sweden. SKB R-02-42. 116 pp. Svensk Kärnbränslehantering AB.

**Alm E, Sundblad K, Huhma H, 2005.** Sm-Nd isotope determinations of low-temperature fluorite-calcite-galena mineralization in the margins of the Fennoscandian Shield. SKB R-05-66. 58 pp. Svensk Kärnbränslehantering AB.

**Bassett M G, 1985.** Silurian stratigraphy and facies development in Scandinavia. In,1985, The Caledonide Orogen; Scandinavia and related areas; Vol 1. p. John Wiley & Sons, Chichester, United Kingdom.

**Bath A, Milodowski A, Ruotsalainen P, Tullborg E-L, Cortés Ruiz A, Aranyossy J-F, 2000.** Evidences from mineralogy and geochemistry for the evolution of groundwater systems during the quaternary for use in radioactive waste repository safety assessment (EQUIP project). pp. EUR report 19613.

**Brownlow A H, 1996.** Geochemistry, Second edition. Prentice Hall. New Jersey, United States of America, 580 pp.

**Canfield B E**, **2001.** Biogeochemistry of sulphur isotopes., Rev Mineral, 43, p. 607–636.

**Carlsson L, Holmqvist A**, **1968.** Ett nytt fynd av sandstensgångar i Västervikstrakten., GFF, 90, p. 519–528.

**Cederbom C, Larson S Å, Tullborg E-L, Stiberg J P**, **2000.** Fission track thermo-chronology applied to Phanerozoic thermotectonic events in central and southern Sweden, Tectonophysics, 316, p. 153–167.

**Chambers L A, Trudinger P A, Smith J W, Burns M S**, **1976.** A possible boundary condition in bacterial sulfur isotope fractionation, Geochimica et Cosmochimica Acta, 40, p. 1191–1194.

**Cole R D, Picard M D, 1981.** Sulfur-isotope variations in marginal-lacustrine rocks of the Green River Formation, Colorado and Utah. In,1981, Recent and ancient nonmarine depositional environments; models for exploration. 31. p. 261–275. SEPM (Society for Sedimentary Geology), Tulsa, OK, United States

**Drake H, Tullborg E-L, 2004.** Fracture mineralogy and wall rock alteration, results from drill core KSH01A+B. SKB P-04-250. 120 pp. Svensk Kärnbränslehantering AB.

**Drake H, Tullborg E-L, 2005.** Fracture mineralogy and wall rock alteration, results from drill cores KAS04, KA1755A and KLX02. SKB P-05-174. 69 pp. Svensk Kärnbränslehantering AB.

**Drake H, Tullborg E-L, 2006a.** Fracture mineralogy, Results from drill core KSH03A+B. SKB P-06-03. Svensk Kärnbränslehantering AB, Submitted to SKB.

**Drake H, Tullborg E-L, 2006b.** Mineralogical, chemical and redox features of red-staining adjacent to fractures, Results from drill cores KSH01A+B and KSH03A+B. SKB P-06-01. Svensk Kärnbränslehantering AB, Submitted to SKB.

**Drake H, Tullborg E-L, in manuscript.** Fracture mineralogy, results from drill cores KLX03, KLX04, KLX05, KLX06, KLX07A+B, KLX08 and KLX10A. P-XX-XX. Svensk Kärnbränslehantering AB.

**Drake H, Tullborg E-L, unpublished data.** Fracture mineralogy investigations of drill cores KA1755A and KAS17. Svensk Kärnbränslehantering AB.

**Field C W, Fifarek R H, 1985.** Light stable-isotopes systematics in the epithermal environment. In,1985, Geology and geochemistry of epithermal systems. 2. p. 99–128. Society of Economic Geologists, Socorro, NM, United States

**Gaal G, Gorbatschev R, 1987.** An outline of the Precambrian evolution of the Baltic Shield. In,1987, Precambrian geology and evolution of the central Baltic Shield; 1st Symposium on the Baltic Shield. 35. p. 15–52. Elsevier, Amsterdam, International

**Harrison A G, Thode H G**, **1957.** Kinetic isotope effect in chemical reduction of sulphate., Faraday Soc Trans, 53, p. 1648–1651.

**Hoefs J, 2004.** Stable Isotope Geochemistry; 5th rev. and updated ed. Springer-Verlag Berlin, Heidelberg, New York. 244 pp.

**Jorgensen B B, Isaksen M F, and Jannasch H W, 1992.** Bacterial sulfate reduction above 100 degrees C in deep-sea hydrothermal vent sediments, Science, 258, p. 1756–1757.

**Kiyosu Y, Krouse H R, 1990.** The role of organic acid in the abiogenic reduction of sulfate and the sulfur isotope effect, Geochemical Journal, 24, p. 21–27.

**Krauskopf K B, Bird D K, 1995.** Introduction to Geochemistry, third edition. McGraw-Hill Book Co. Singapore. 647 pp.

**Kresten P, Chyssler J**, **1976.** The Götemar Massif in south-eastern Sweden; a reconnaissance survey, Geologiska Föreningen i Stockholm Förhandlingar, 98, Part 2, p. 155–161.

**Laaksoharju M, Smellie J, Gimeno M, Auqué L, Gómez J, Tullborg E-L, Gurban I, 2004.** Hydrogeochemical evaluation of the Simpevarp area, model version 1.1. SKB R-04-16. 398 pp. Svensk Kärnbränlsehantering AB.

**Larson S Å, Tullborg E-L, Cederbom C, Stiberg J P**, **1999a.** Sveconorwegian and Caledonian foreland basins in the Baltic Shield revealed by fission-track thermochronology, Terra Nova, 11, p. 210–215.

**Larson S Å, Tullborg E-L, Cederbom C, Stiberg J P, Plink B P, Bjorklund L, 1999b.** The Caledonian foreland basin in Scandinavia; constrained by the thermal maturation of the Alum Shale; discussion and reply, GFF, 121, p. 155–159.

**Machel H G, Krouse H R, Sassen R, 1995.** Products and distinguishing criteria of bacterial and thermochemical sulfate reduction, Applied Geochemistry, 10, p. 373–389.

**McKay J L, Longstaffe F J, 2003.** Sulphur isotope geochemistry of pyrite from the Upper Cretaceous Marshybank Formation, Western Interior Basin, Sedimentary Geology, 157, p. 175–195.

**McKibben M A, Eldridge C S, 1994.** Micron-scale isotopic zoning in minerals; a record of large-scale geologic processes, Mineralogical Magazine, 58A, p. 587–588.

**Milodowski A E, Tullborg E-L, Buil B, Gomez P, Turrero M-J, Haszeldine S, England G, Gillespie M R, Torres T, Ortiz J E, Zacharias, Silar J, Chvatal M, Strnad L, Sebek O, Bouch, Jesr Chenery1 C, Chenery C, Sheperd T J, 2005.** Application of Mineralogical, Petrological and Geochemical tools for Evaluating the Palaeohydrogeological Evolution of the PADAMOT Study Sites. PADAMOT Project Technical Report WP2. pp.

**Nordenskjöld C E, 1944.** Morfologiska studier inom overgangsomradet mellan Kalmarslatten och Tjust.Medd. Lunds Univ. Geog. Inst. Avh. VIII.

**O'Neil J R, Clayton R N, and Mayeda T K, 1969.** Oxygen isotope fractionation in divalent metal carbonates, Journal of Chemistry and Physics, 51, p. 5547–5558.

**Ohmoto H, 1972.** Systematics of Sulfur and Carbon Isotopes in Hydrothermal Ore Deposits, Economic Geology and the Bulletin of the Society of Economic Geologists, 67, p. 551–578.

**Ohmoto H, Rye R O, 1979.** Isotopes of sulfur and carbon; 2. In,1979, Geochemistry of hydrothermal ore deposits. p. John Wiley & Sons, New York, NY, United States

**Ohmoto H, Goldhaber M B, 1997.** Sulfur and carbon isotopes; 3. In,1997, Geochemistry of hydrothermal ore deposits. p. John Wiley & Sons, New York, NY, United States

**Orr W L, 1974.** Changes in Sulfur Content and Isotopic Ratios of Sulfur during Petroleum Maturation; Study of Big Horn Basin Paleozoic Oils. In,1974, Advances in Petroleum Geochemistry. 58; 11, Part 1. p. 2295–2318. American Association of Petroleum Geologists, Tulsa, OK, United States

**Robinson B W, Kusakabe M, 1975.** Quantitative preparation of sulphur dioxide for 34S/32S analyses from sulphides by combustion with cuprous oxide., Analytical Chemistry, 47, p. 1179–1181.

**Röshoff K, Cosgrove J, 2002.** Sedimentary dykes in the Oskarshamn-Västervik area – A study of the mechanism of formation. SKB R-02-37. 98 pp. Svensk Kärnbränslehantering AB.

**SKB, 2005.** Preliminary site description, Simpevarp subarea – version 1.2. SKB R-05-08. 589 pp. Svensk Kärnbränlsehantering AB.

**Smellie J A T, Stuckless J S, 1985.** Element mobility studies of two drill-cores from the Goetemar Granite (Kraakemaala test site), Southeast Sweden, Chemical Geology, 51, p. 55–78.

**Sollien D, 1999.** Control of fluorite-galena-bearing fractures and clastic sandstones dykes in the Tindered area, south-eastern Sweden. Project work, Norwegian University of Science and Technology, Trondheim. p. 26.

**Sundblad K, Alm E, Huhma H, Vaasjoki M, and Sollien D B, 2004.** Early Devonian tectonic and hydrothermal activity in the Fennoscandian Shield; evidence from calcite-fluorite-galena mineralization, In: Mertanen S (ed), Extended abstracts, 5th Nordic Paleomagnetic workshop. Supercontinents, remagnetizations and geomagnetic modelling., Geological Survey of Finland, p. 67–71.

**Sundblad K A E, 2000.** Flusspatforande spricksystem i den prekambriska berggrunden i Ostersjoregionen., Institutionen for geologi och geokemi Stockholms universitet.

**Trudinger P A, Chambers L A, Smith J W, 1985.** Low-temperature sulphate reduction; biological versus abiological. In,1985, Role of organisms and organic matter in ore deposition – Le role des organismes et de la matiere organique dans la formation des gisements metalliferes. 22; 12. p. 1910–1918. National Research Council of Canada, Ottawa, ON, Canada

**Tullborg E-L, 1988.** Fracture fillings in the drillcores from Äspö and Laxemar. In: Wikman.H., Kornfält, K.-A., Riad, L., Munier, R., Tullborg E.-L., 1988: Detailed investigations of the drillcores KAS02, KAS03 and KAS04 on Äspö Island and KLX01 at Laxemar. SKB PR 25-88-11. 30 pp. Svensk Kärnbränslehantering AB.

**Tullborg E-L, 1997.** Recognition of low-temperature processes in the Fennoscandian Shield: Doctoral thesis, Earth Science Centre A17, Göteborg University, 35 pp.

**Tullborg E-L**, **2004.** Palaeohydrogeological evidences from fracture filling minerals. Results from the Äspö/Laxemar area., Mat. Res.Soc. Symp., Vol 807, p. 873–878.

**Tullborg E-L, Larson S Å, Stiberg J P, 1996.** Subsidence and uplift of the present land surface in the southeastern part of the Fennoscandian Shield, GFF, p. 126–128.

**Wallin B, Peterman Z, 1999.** Calcite fracture fillings as indicators of palaeohydrogeology at Laxemar at the Äspö Hard Rock Laboratory, southern Sweden., Applied Geochemistry, Vol. 14, p. 953–962.

**Zeck H P, Andriessen P A M, Hansen K, Jensen P K, Rasmussen B L, 1988.** Paleozoic paleo-cover of the southern part of the Fennoscandian Shield; fission track constraints, Tectonophysics, 149, p. 61–66.

**Åberg G, 1978.** A geochronological study of the Precambrian of southeastern Sweden. Geologiska Föreningens i Stockholm Förhandlingar, 100, p. 125–154.

**Åberg G, Löfvendahl R, Levi B, 1984.** The Götemar granite-isotopic and geochemical evidence for a complex history of an anorogenic granite, Geologiska Föreningen i Stockholm Förhandlingar, 106, p. 327–333.

**Åhäll K-I, 2001.** Åldersbestämning av svårdaterade bergarter i sydöstra Sverige. SKB R-01-60. 28 pp. Svensk Kärnbränslehantering AB.

# Appendix 1

## Sample descriptions, KKR01

### KKR01: 153.40–153.50 m

Sample type: Surface sample.
Rock type: Götemar granite.
Fracture: Open fracture with a one millimetre thick, fine-grained, bright coating.

Minerals: Albite, Calcite, Quartz, Fluorite, K-feldspar, Muscovite, (possibly Laumontite).

The surface is covered by a pink layer and a whitish layer which seem to be coeval, although the whitish layer might be formed later than the pink layer.

The pink layer consists of quartz, calcite, albite, muscovite, K-feldspar (possibly adularia) and a single crystal that might be laumontite.

The white layer consists of calcite ($MnO_2$ = 0.95–1.20%), muscovite and fluorite (sometimes euhedral).

### KKR01: 157.30–157.45 m

Sample type: Surface sample.
Rock type: Götemar granite.
Fracture: Thin fracture coating of fine-grained crystals as well as fragments from the wall rock. Some parts of the fracture are even more fine-grained and white to grey in colour. This coating is also present in sealed fractures that are penetrating about one centimetre into the wall rock.

The fragments in the filling are made up of wall rock minerals, mainly quartz, K-feldspar, albite and subordinately muscovite and biotite. The fine-grained material is dominantly quartz but Fe-rich chlorite and K-feldspar crystals are also present. The white to grey coloured filling consists of a thin cover of minute quartz crystals.

### KKR01: 163.70–163.75 m

Sample type: Surface sample.
Rock type: Götemar granite.
Fracture: Millimetre thick reddish brown coating. The coating is also present in sealed fractures in the wall rock.

Calcite, quartz and muscovite are equally present in the sample. Some small hematite grains are present. Small but measurable (~1%) amounts of FeO are present in most of the analysed minerals on the fracture surface. This Fe is thought to give the fracture coating its distinct red colour.

## KKR01: 492.75–492.80 m

Sample type: Thin section.
Rock type: Götemar granite.
Fracture: 1–2 mm wide, associated fractures with similar orientation (only one is visible in the thin section). The fracture filling is brown and wall rock fragments are abundant. There are some minor fractures running parallel to the major fracture in the thin section.

Minerals in the filling matrix: Quartz, Fluorite, Adularia, Hematite, ML-clay (possibly chlorite + illite), Muscovite,

The main minerals in the matrix of the filling in between the wall rock fragments are quartz and fluorite. It is hard to distinguish if the fluorite crystals are earlier formed fragments or if they are coeval with quartz. There are also some aggregates of hematite, ML-clay (possibly chlorite + illite) and muscovite in the quartz-matrix. These hematite crystals are probably formed in voids, which are very common, in the quartz filling.

The two micro-fractures that are running parallel to the main fracture are filled with quartz/fluorite and adularia/quartz/fluorite, respectively.

*Thin section "KKR01 – 492.75–492.80 m" scanned with plain polarized light. The thin section is about 4 cm wide.*

# Appendix 2

## Sample descriptions, KKR02

### KKR02: 23.12–23.25 m

Sample type: Surface sample.
Rock type: Götemar granite.
Fracture: Open fracture with a millimetre thick, fine-grained, white to light green coloured coating.

Calcite ($MnO_2$ = 1–1.15%, FeO = 0.5%) is the only mineral present on the fracture surface and is covering the surface as a thin layer.

### KKR02: 95.75–95.95 m

Sample type: Surface sample.
Rock type: Götemar granite.
Fracture: Originally 1–2 mm thick sealed fracture (opened during sample preparation – cutting). The colour of the fracture filling is bright red to brown. The surface of the newly opened fracture was examined.

Minerals: Quartz, Calcite, Pyrite, U-silicate, Galena, Fluorite.

Quartz and calcite dominate the fracture coatings. The analyses of calcite and quartz crystals show 1–2% FeO, inferring that micro crystals of Fe-oxide are present. This gives the red colour to the filling.

Some parts of the filling consist of U-rich silicate in paragenesis with some galena crystals. Pyrite crystals are present more or less evenly in the sample. Some euhedral fluorite crystals are also present.

### KKR02: 159.92–159.95 m

Sample type: Surface sample.
Rock type: Götemar granite.
Fracture: Open fracture with an up to 5 mm thick coating, which consists of angular wall rock fragments (< 1 mm in diameter) and more fine-grained “cement”. The coating is mostly beige in colour and the fragments are mostly red or grey.

Bright coloured, fine-grained parts of the filling are dominantly made up of quartz crystals. The most common minerals in the fragments are quartz, K-feldspar and albite. Some fragments of denser minerals, dominantly Ti-Fe-rich oxides and monazite and subordinately galena are also present.

### KKR02: 171.52–171.61 m

Sample type: Surface sample.
Rock type: Götemar granite.
Fracture: Open fracture with a thin (< 1 mm) coating, covering about 50% of the surface. The coating is white to yellowish white.

Minerals: Calcite, U-silicate, Fluorite, Zircon.

The fracture surface is covered by a thin white layer of dominantly calcite. Very small amounts of U-silicate, fluorite and zircon are also present.

### KKR02: 236.69–236.84 m

Sample type: Surface sample.
Rock type: Götemar granite.
Fracture: Open fracture with fluorite next to the wall rock and calcite crystals on top of the fluorite crystals.

Minerals: Fluorite, Calcite, Pyrite, Galena, Chalcopyrite

Fluorite and calcite dominate the fracture filling and pyrite, galena and chalcopyrite are present on top of the calcite crystals. Pyrite is the most abundant sulphide in this sample.

### KKR02: 258.24–258.41 m

Sample type: Surface sample.
Rock type: Götemar granite.
Fracture: Mainly open fracture, parallel to the drill core axis. A part of the fracture (not examined in the surface sample) is sealed and purple in colour due to fluorite. The fracture surface of the open fracture consists of a very thin, fine-grained green cover and bigger euhedral fluorite and quartz crystals visible macroscopically. Some parts of the surface sample expose the wall rock with coarse-grained minerals of quartz and feldspar. The fracture surfaces of the open fractures look similar on both sides.

Minerals: Fluorite, Chlorite, Quartz

The fine-grained, green coloured fracture coating consists of euhedral platy crystals of Fe-rich chlorite and euhedral cubic crystals of fluorite. More coarse-grained euhedral crystals of quartz and fluorite are abundant on the surface. The three minerals are probably formed synchronously.

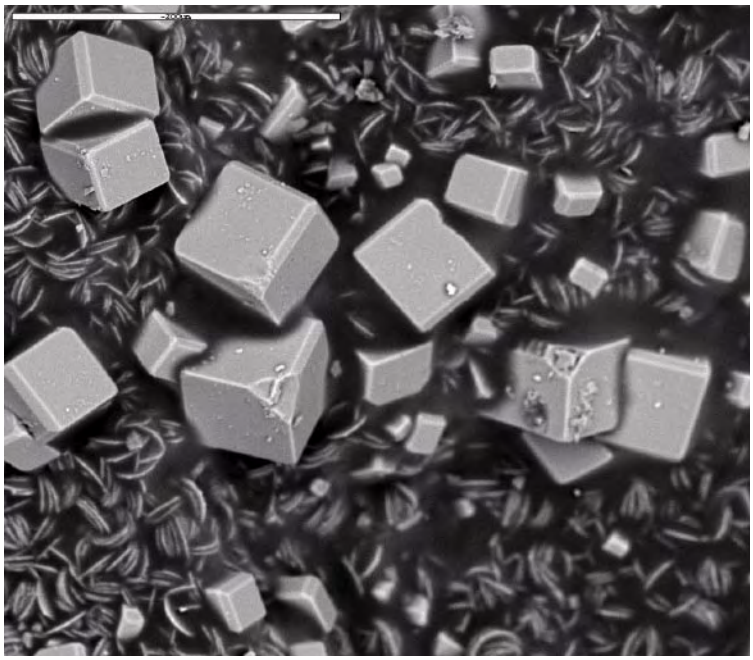

*Back-scattered SEM-image of cubic fluorite crystals and platy Fe-rich chlorite crystals. Scale bar is 200 µm.*

## KKR02: 367.58–367.73 m

Sample type: Surface sample.
Rock type: Götemar granite.
Fracture: Open fracture, parallel to the drill core axis. The fracture surface contains a very thin dark cover and euhedral fluorite and quartz crystals visible macroscopically. The wall rock, with coarse-grained minerals of quartz and feldspar, is exposed in some parts of the surface sample. The fracture surfaces look similar on both of the walls.

Minerals: Fluorite, Chlorite, Quartz, Galena, Pyrite, Calcite, REE-carbonate, Hematite, Cu-oxide, Apatite

The fine-grained, green coloured fracture coating consists of euhedral platy crystals of Fe-rich chlorite and euhedral cubic crystals of fluorite. More coarse-grained euhedral crystals of quartz and fluorite are abundant on the surface. These three minerals are thought to have formed at the same event.

Some crystals of galena, calcite, pyrite, REE-carbonate, hematite, apatite and Cu-oxide are also present in this sample.

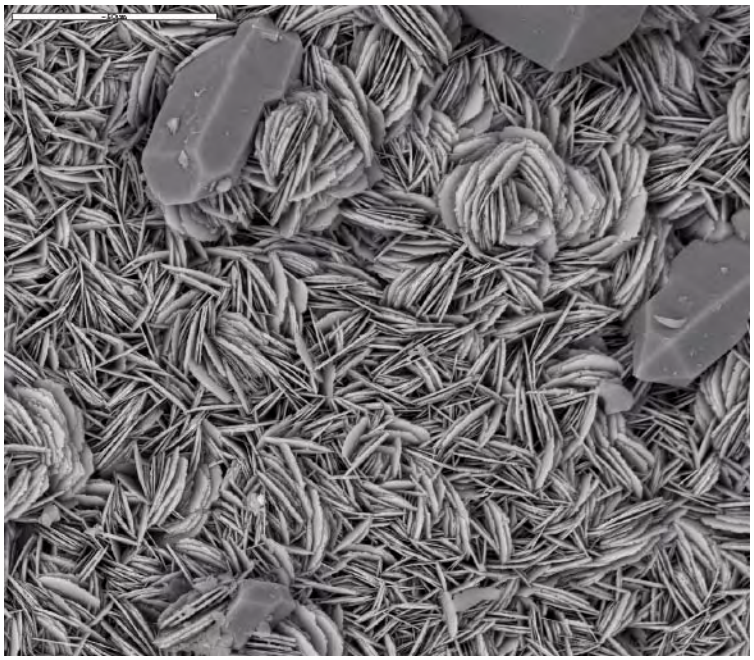

*Back-scattered SEM-image of euhedral quartz crystals and platy, more fine-grained, Fe-rich chlorite crystals. Scale bar is 200 µm.*


*Back-scattered SEM-image of euhedral fluorite crystals (Fl), quartz crystals (Qz) and platy, more fine-grained, Fe-rich chlorite crystals (Chl).*

# Appendix 3

## Sample descriptions, KKR03

### KKR03: 52.25–52.37 m

Sample type: Thin section.
Rock type: Götemar granite.
Fracture: 8 mm wide sealed fracture with fluorite next to the wall rock and calcite in the middle of the fracture. Calcite is the most abundant mineral. Some parts of the fracture filling are red/brown-stained. The fracture filling is somewhat porous with some minute, irregularly distributed voids.

Minerals: Calcite, Fluorite, Fe-oxide, Sphalerite, Pyrite, Barite, U-silicate, Chlorite

Order: The minerals in the filling seem to be of essentially the same age. At least calcite and fluorite are most likely coeval. Sphalerite, Fe-oxide and pyrite are found in crystals of fluorite and calcite and often occupy voids. Sphalerite and Fe-oxide (possibly hematite) appear dominantly in the part of the sample that is red/brown in hand-sample. Crystals of barite, U-silicate, and Fe-rich chlorite are also present in the filling.

Wall rock alteration: The wall rock alteration in this sample is gentle.

### KKR03: 54.83–54.86 m

Sample type: Surface sample.
Rock type: Götemar granite.
Fracture: Open fracture covered by an up to 1 cm thick, porous filling of dominantly euhedral fluorite and calcite crystals.

Minerals: Fluorite, Calcite, Chlorite, Pyrite, Galena, Hematite, Quartz, Cu-oxide, (REE-carbonate), (Barite), (Adularia), (Wolframite)

The euhedral fluorite crystals often have euhedral pyrite on their surfaces. Euhedral calcite and fluorite are of essentially the same age, although the fluorite is present next to the wall rock. Some parts of the sample are more calcite-rich and some are more fluorite-rich. Some euhedral quartz crystals are also present.

Fe-rich chlorite appears as a green coloured cover on fluorite crystals. Also present are small crystals of galena, hematite, Cu-oxide, REE-carbonate, adularia, barite and a W-rich mineral (possibly wolframite).

### KKR03: 75.20–75.30 m

Sample type: Surface sample.
Rock type: Götemar granite.
Fracture: Partly sealed fracture dominated by fluorite, calcite and galena.

Minerals: Fluorite, Calcite, Galena, Pyrite, Chlorite, Hematite, Barite, Quartz, U-silicate

Fluorite is coating the fracture wall while calcite, galena and pyrite are visible macroscopically in the middle of the fracture. Smaller crystals of Fe-rich chlorite, barite, hematite, quartz and U-silicate are also present.

## KKR03: 251.83–251.85 m

Sample type: Thin section (100 µm thick).
Rock type: Götemar granite.
Fracture: Open fracture with a 5 mm thick coating. The coating is mostly green in colour with subordinate yellowish green parts.

Minerals: Muscovite, Illite (possibly in mixed layer-clay with chlorite), Chlorite, Pyrite, Hematite

Order:

1. Muscovite.
2. Illite (no certain identification), possibly with minor amounts of chlorite (in Mixed-layer clay).
3. Fe-rich chlorite ($Fe_2O_3$ = 36–41%, MgO = 5–6%) is often filling fractures that are cutting trough muscovite and is present in voids of the muscovite and subordinately in voids of the illite filling.

Hematite crystals are present in voids of the muscovite filling and are therefore formed later than muscovite. No relation has been found between hematite and illite. Some euhedral as well as subhedral pyrite crystals are found in the muscovite filling as well.

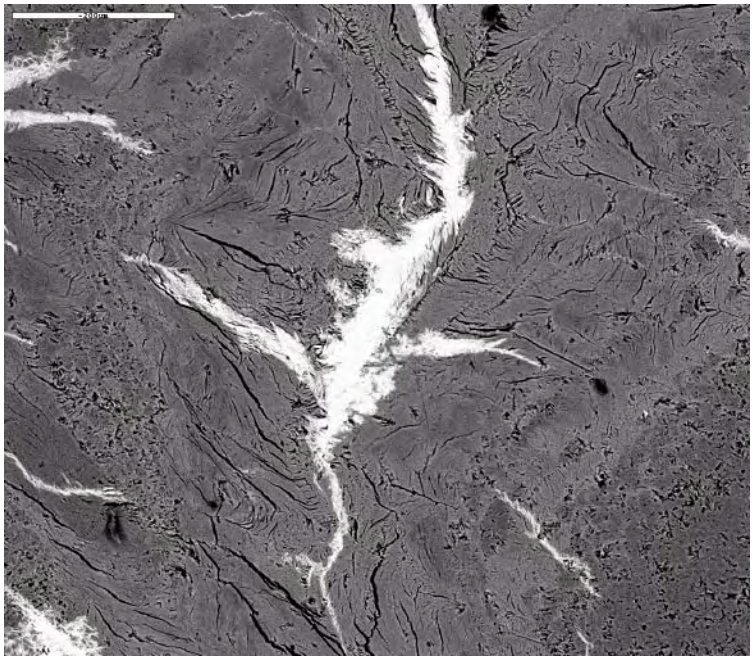

*Back-scattered SEM-image of Fe-rich (white) chlorite present in a muscovite filling (grey). The chlorite is probably formed later than the muscovite but the timing can not be distinguished. Scale bar is 200 µm.*

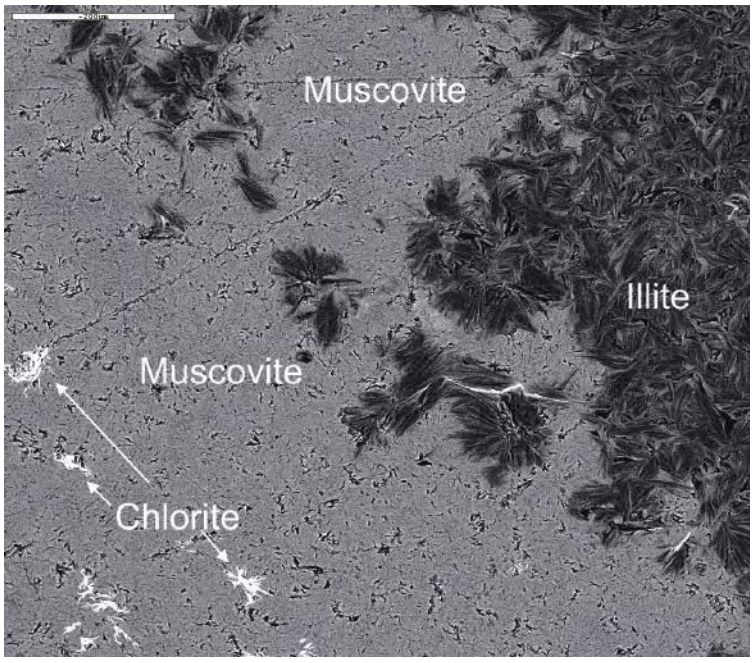


*Back-scattered SEM-image of Fe-rich chlorite present in a muscovite-illite filling. Scale bar is 200 µm.*

## KKR03: 258.23–258.34 m

Sample type: Surface sample.
Rock type: Götemar granite.
Fracture: Open fracture with a 1–2 mm thick purple coating with euhedral fluorite crystals, easily visible macroscopically. Some parts of the coating are white coloured and consist of calcite.

Minerals: Fluorite, Quartz, Chlorite, Calcite, Chalcopyrite, Hematite, U-silicate, REE-carbonate, Cu-oxide, (Wolframite)

Euhedral cubic fluorite is the most abundant mineral in this coating. Related minerals are euhedral Fe-rich chlorite (platy), quartz, calcite and pyrite. The latter is occasionally present on the surfaces of fluorite crystals. Some crystals of chalcopyrite, hematite, U-silicate, REE-carbonate, Cu-oxide and a W-rich mineral (possibly wolframite) are also found grown on surfaces of fluorite crystals.

A part of the sample is covered with calcite with pyrite crystallised on the crystal surfaces.

*Back-scattered SEM-image of mostly cubic fluorite crystals of variable size. Minor amounts of darker quartz crystals and platy Fe-rich chlorite crystals. Scale bar is 200 µm.*

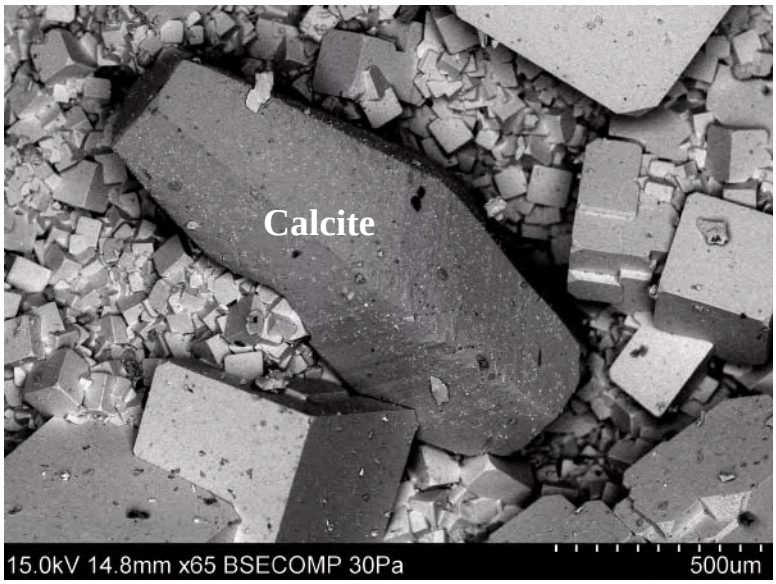


*Back-scattered SEM-image of cubic fluorite crystals of variable size and a single scalenohedral calcite crystal.*

## KKR03: 336.62–336.72 m

Sample type: Surface sample.
Rock type: Götemar granite.
Fracture: Partly sealed fracture dominated by fluorite and calcite.

Minerals: Fluorite, Calcite, Pyrite, Galena, Quartz, Chlorite, Barite, Adularia, Hematite, REE-carbonate

Fluorite is coating the fracture while calcite is visible in the middle of the fracture. Smaller crystals of Fe-rich chlorite, pyrite, galena, quartz, barite, adularia, hematite and REE-carbonate are also present.

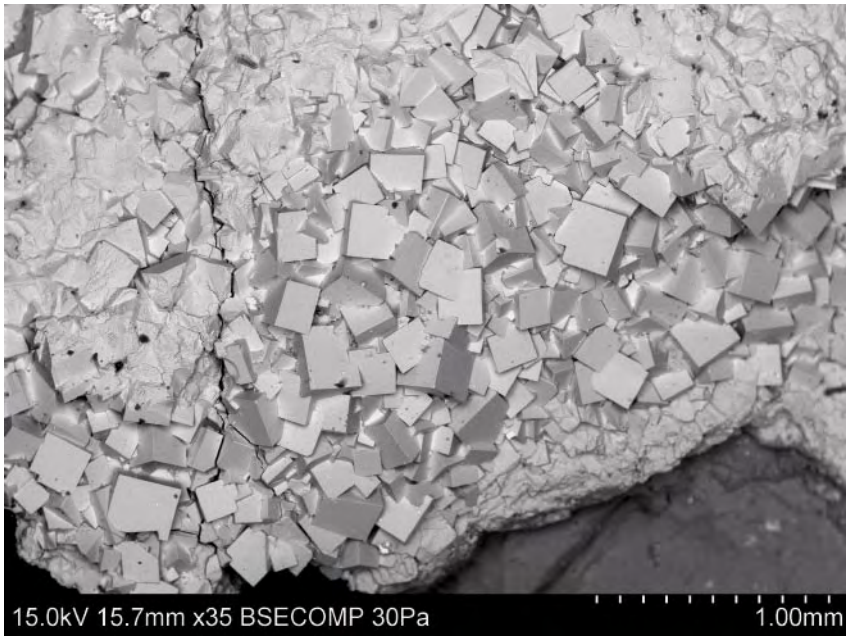


*Back-scattered SEM-image of cubic fluorite crystals of variable size.*

## KKR03: 389.11–389.13 m

Sample type: Surface sample.
Rock type: Götemar granite.
Fracture: Open fracture with a thin (< 1 mm) coating, covering half of the surface. The coating is white to yellowish white. Small crystals of scalenohedral calcite are visible macroscopically.

Minerals: Calcite, Pyrite, Adularia, Albite

The fracture surface is covered with euhedral scalenohedral calcite crystals growing perpendicular to the surface. Euhedral ~20 µm pyrite crystals, along with fine-grained adularia and albite, are growing on, and in between, the calcite crystals.

*Back-scattered SEM-image of bright pyrite crystals on the surface of a calcite crystal. Scale bar is 20 µm.*

### KKR03: 539.04–539.12 m

Sample type: Surface sample.
Rock type: Götemar granite.
Fracture: Open fracture with a 1–2 mm thick coating. The sample coating is white to purple in colour due to the presence of calcite and fluorite, respectively. The wall rock granite is visible in some parts of the sample.

Minerals: Fluorite, Calcite, Quartz, Pyrite, Chlorite, Galena, Sphalerite, REE-carbonate, Hematite, Cu-oxide

The majority of the sample consists of euhedral cubic fluorite crystals and euhedral calcite crystals. In some parts of the sample euhedral crystals of quartz are found in paragenesis with fluorite. Fe-rich chlorite also appears in the sample, e.g. on euhedral quartz crystals. Euhedral and subhedral pyrite crystals are found on the surfaces of fluorite, calcite and quartz, irregularly throughout the coating.

A thin green cover of mainly Fe-rich chlorite (probably with clay minerals) is found on some of the fluorite crystals. Some crystals of galena, sphalerite, REE-carbonate, hematite and Cu-oxide are also found on the fracture surface. These minerals seem to be coeval with calcite, quartz and fluorite.

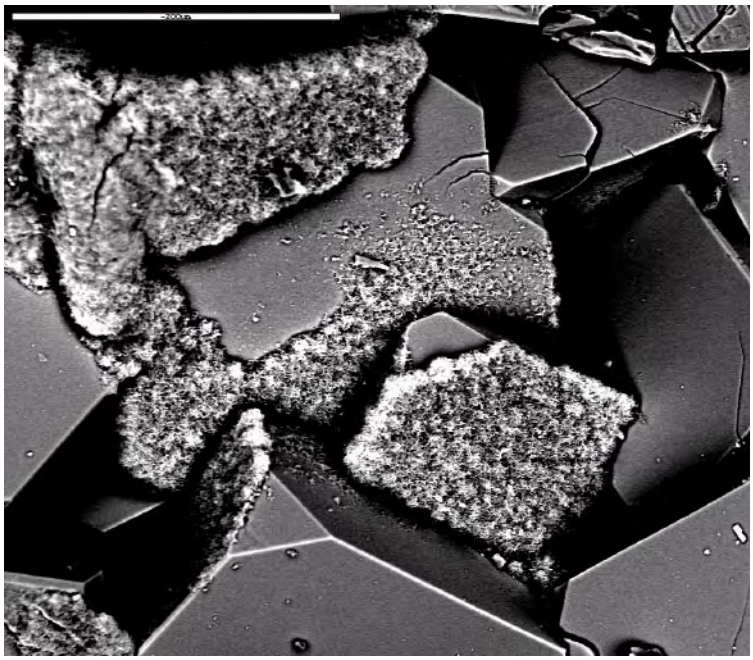

*Back-scattered SEM-image of fine-grained, Fe-rich chlorite on the surfaces of cubic fluorite crystals. Scale bar is 200 µm.*

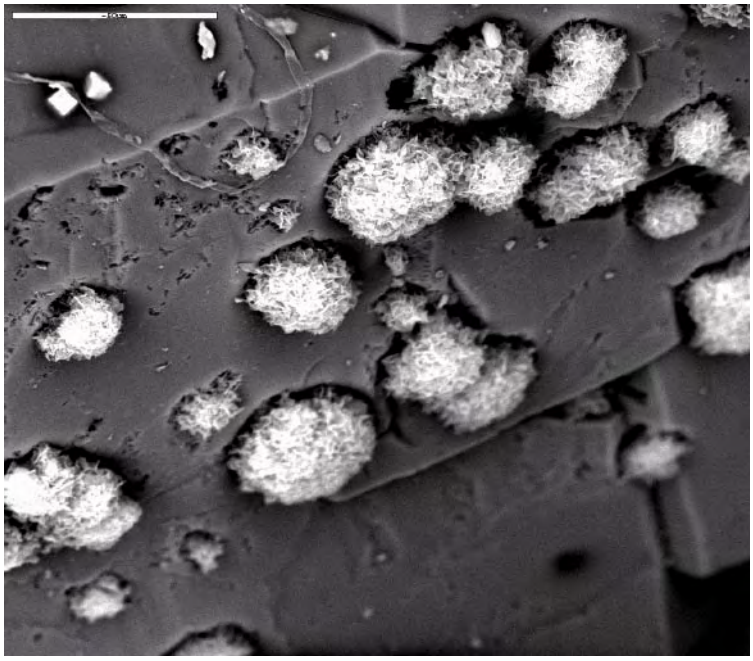

*Back-scattered SEM-image of fine-grained, Fe-rich chlorite on the surface of a quartz crystal. Scale bar is 50 µm.*

## KKR03: 651.75–651.79 m

**Sample type:** Thin section (100 micron thick).
**Rock type:** Götemar granite.
**Fracture:** 5 cm wide zone of porous and altered wall rock. Voids in between crystals are filled with a fine-grained, light orange coloured filling. The sample resembles a fragment-dominated breccia.

**Minerals:** Albite, Chlorite, Muscovite

Breccia sealing consists mostly of albite and some crystals of Fe-chlorite (FeO = 24%, MgO = 9%) and muscovite.

## KKR03: 733.55–733.58 m

Sample type: Thin section.
Rock type: Götemar granite.
Fracture: 1–2 cm wide, porous zone of breccia with coarse-grained, often tabular, wall rock fragments and a fine-grained, dark green matrix.

Minerals: Chlorite, Muscovite, Hematite, K-feldspar (possibly adularia), Quartz.

The fine-grained matrix consists of Fe-rich chlorite, muscovite, hematite, K-feldspar (possibly adularia) and quartz.

Part of this matrix is brownish (somewhat reddish) and consists of a higher amount of Fe-rich chlorite (with higher FeO, about 35%) and hematite than in the rest of the matrix. However, in general the hematite-content is rather low.

The brighter parts of the fine-grained filling are usually more muscovite rich.

The angular fragments are commonly K-feldspar, quartz and albite originating from the wall rock.

# Appendix 4

## Sample descriptions, Sandstone

### Sandstone (I) from the Kråkemåla quarry #2:

**Sample type:** Thin section.

**Sample description:**

The sandstone fracture is about one centimetre wide and borders to fluorite filled fractures running parallel to the sandstone. The fluorite filling contains a couple of angular fragments of the wall rock granite.

The sandstone is dominantly made up of rounded quartz clasts with minor amounts (< 10% of the clasts) of more angular K-feldspar crystals, possibly derived from the wall rock. The cement is dominantly made up of fluorite but subordinate fine-grained quartz and K-feldspar exist. The clasts are commonly surrounded by the fluorite cement.

The fluorite filling next to the sandstone contain some rounded clasts of quartz and some more angular clasts of K-feldspar. These crystals appear close to the contact to the fracture filling-sandstone and are thought to originate from this. This indicates that the fluorite filling is formed later than the sandstone.

There is no obvious trend in the distribution of rounded versus angular clasts and coarse-grained versus fine-grained clasts in the sandstone. The clasts become more fine-grained closer to one of the wall-rock contacts, but the clasts bordering the opposite wall-rock contact are coarse-grained and rounded. A couple of angular and more coarse-grained clasts or fragments are found in the middle of the sandstone filled fracture.

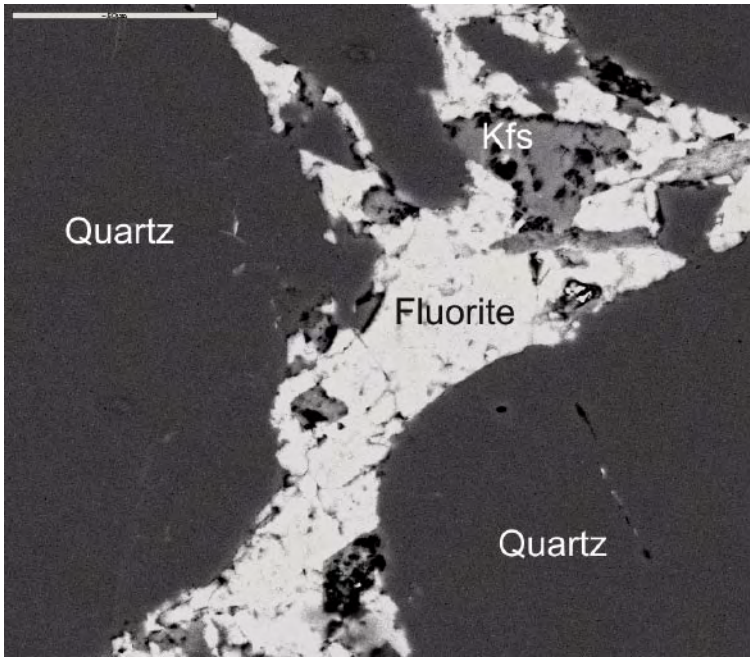


*Back-scattered SEM-image of rounded quartz clasts, angular K-feldspar grains (Kfs) and cement of fluorite. Quartz and K-feldspar are slightly dissolved, suggesting that fluorite filled the pore-space after the sandstone was consolidated. Scale bar is 50 µm.*

## Sandstone (II) from the Kråkemåla quarry #2:

**Sample type:** Thin section.

**Sample description:**

The sandstone fracture is about one centimetre wide in the thin section and borders to granitic wall rock and fluorite filled fractures on both sides of the filling. Sometimes the fluorite filled fractures show angular fragments of the wall rock.

The sandstone is dominantly made up of rounded quartz clasts with minor amounts (< 10% of the clasts) of more angular K-feldspar crystals, possibly derived from the wall rock. The sample differs from sample (I) such that the sandstone can be divided into two parts with different texture. One is similar to that in sample (I) where the cement is dominantly made up of fluorite, but subordinate fine-grained quartz and K-feldspar exist. The other has a higher amount of fine-grained quartz and K-feldspar and a lower amount of fluorite as cement, although fluorite dominates the cement. The clasts are as in sample (I) usually surrounded by the fluorite cement. There are no obvious trends in the distribution of rounded versus angular clasts and coarse-grained versus fine-grained clasts in the thin section. The clasts become more fine-grained to one of the wall-rock contacts, but the clasts bordering the opposite wall-rock contact are coarse-grained and rounded. Angular and more coarse-grained clasts and fragments are occasionally found in the middle of the sandstone filled fracture. These clasts are however found in a section of very fine-grained clasts.

The fluorite filling next to the sandstone contains less clasts of quartz and K-feldspar than in sample (I) but the fluorite gives the impression of being formed after the formation of the sandstone in this sample as well.

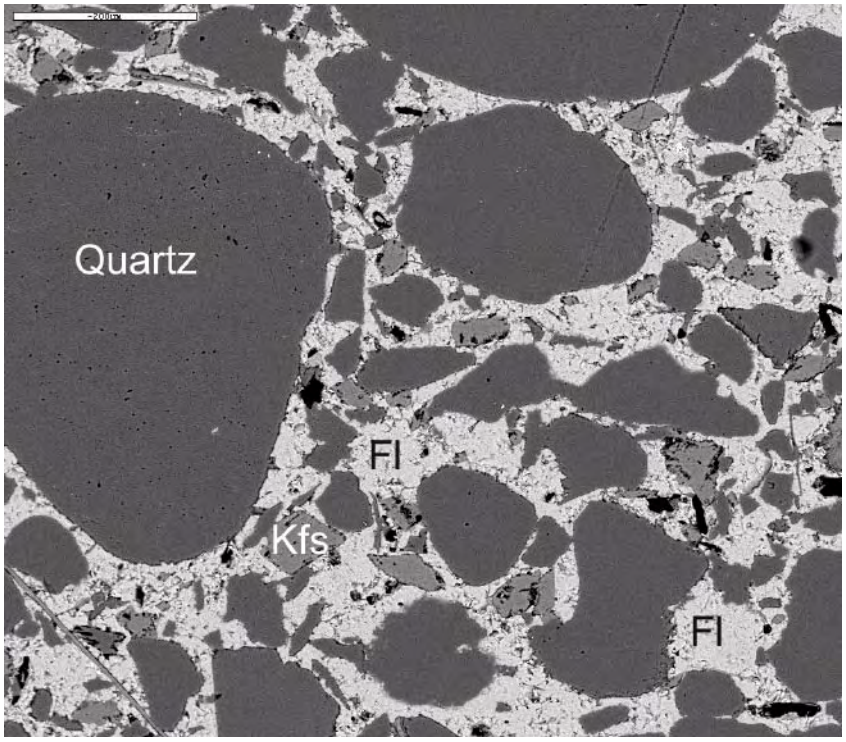


*Back-scattered SEM-image of mostly rounded quartz clasts, angular K-feldspar grains (Kfs) and cement of fluorite (Fl). Scale bar is 200 µm.*

# Appendix 5

## SEM-EDS analyses

Detection limit of SEM-EDS is about 0.3% for $Na_2O$ and about 0.1% for other oxides. Where no result is shown the element was below the detection limit. Elements like S and Zn yield too high values, which result in total values of higher than 100 per cent. The SEM-EDS analyses give values of the total Fe-content, distinctions of Fe(II) and Fe(III) can not be made.

| Sphalerite | $SO_3$ | CaO | ZnO | $MoO_3$ | CdO | Total |
|---|---|---|---|---|---|---|
| KKR03 – 52.25–52.37 | 74.62 | 1.48 | 80.95 | 2.24 | 1.61 | 160.91 |

| Fe-rich chlorite | MgO | $Al_2O_3$ | $SiO_2$ | $K_2O$ | CaO | MnO | FeO | Total |
|---|---|---|---|---|---|---|---|---|
| KKR03 – 52.25–52.37 | 7.48 | 17.95 | 25.7 | | 0.59 | 0.38 | 35.73 | 87.82 |
| KKR03 – 251.83–251.85(1) | 5.84 | 20.67 | 27.65 | 0.41 | | 0.32 | 32.97 | 87.86 |
| KKR03 – 251.83–251.85(2) | 6.29 | 20.04 | 26.51 | 0.20 | 0.21 | 0.30 | 34.97 | 88.52 |
| KKR03 – 251.83–251.85(3) | 4.80 | 18.54 | 24.87 | | | 0.49 | 37.85 | 86.55 |
| KKR03 – 539.04–539.12 | 2.57 | 12.06 | 31.51 | | 5.25 | 0.34 | 37.28 | 89.01 |
| KKR03 – 651.75–651.79(1) | 11.53 | 20.67 | 28.41 | 0.30 | | 0.76 | 27.98 | 89.65 |
| KKR03 – 651.75–651.79(2) | 8.54 | 20.39 | 31.60 | 1.21 | | 0.45 | 24.72 | 86.91 |
| KKR03 – 733.55–733.58(1) | 5.56 | 20.12 | 29.53 | 2.40 | | | 26.13 | 83.74 |
| KKR03 – 733.55–733.58(2) | 8.90 | 19.33 | 30.34 | 1.42 | | 0.27 | 28.17 | 88.43 |

| Muscovite | $Na_2O$ | MgO | $Al_2O_3$ | $SiO_2$ | $K_2O$ | CaO | $TiO_2$ | MnO | FeO | Total |
|---|---|---|---|---|---|---|---|---|---|---|
| KKR03 – 251.83–251.85 | | 2.73 | 27.34 | 51.09 | 10.58 | | | | 3.37 | 95.10 |
| KKR01 – 153.40–153.50(1)* | 0.40 | 2.69 | 29.10 | 51.61 | 10.78 | 0.18 | 0.54 | 0.43 | 5.83 | 101.57 |
| KKR01 – 153.40–153.50(2)* | 2.81 | 0.82 | 25.65 | 63.85 | 6.55 | 0.90 | 0.32 | 0.22 | 3.91 | 104.76 |
| KKR01 – 163.70–163.75* | | 1.18 | 19.34 | 35.80 | 8.78 | 0.32 | 0.47 | 0.98 | 6.34 | 73.21 |
| KKR03 – 651.75–651.79(1) | | 4.14 | 24.84 | 49.53 | 8.61 | | | | 7.52 | 94.63 |
| KKR03 – 651.75–651.79(2) | | 3.50 | 24.92 | 51.18 | 10.15 | | | | 4.26 | 94.00 |
| KKR03 – 733.55–733.58 | | 2.82 | 26.59 | 50.14 | 9.31 | | | 0.22 | 6.97 | 96.05 |

* = Surface sample, no representative analysis.

| Illite (in ML-clay with chlorite) | MgO | $Al_2O_3$ | $SiO_2$ | $K_2O$ | CaO | $Fe_2O_3$ | Total |
|---|---|---|---|---|---|---|---|
| KKR03 – 251.83–251.85(1) | 1.44 | 37.29 | 43.90 | 3.62 | 0.29 | 4.11 | 90.64 |
| KKR03 – 251.83–251.85(2) | 0.69 | 41.16 | 37.53 | 1.07 | | 2.99 | 83.44 |

| Fe-rich material | $Na_2O$ | $Al_2O_3$ | $SiO_2$ | $K_2O$ | CaO | FeO | Total |
|---|---|---|---|---|---|---|---|
| KKR01 – 157.30–157.45 | 0.75 | 1.93 | 36.69 | 0.27 | 0.23 | 47.16 | 87.03 |

# Appendix 6

## Fracture filling sequence form Simpevarp/Laxemar/Äspö

**Schematic fracture filling-sequence from Simpevarp/Laxemar/Äspö/ modified from /Drake and Tullborg 2006/. Bold letters indicate the most abundant minerals in each generation. Minerals in brackets are occasionally identified.**

1. **Quartz-** and **epidote**-rich mylonite**,** occasionally including muscovite, titanite, Fe-Mg-chlorite, albite, (apatite), (calcite), (K-feldspar).
2. Cataclasite.
   - **a.** Early **epidote**-rich, with **quartz**, titanite, Fe-Mg-chlorite, (K-feldspar), (albite).
   - **b.** Late **hematite**-rich, with epidote, **K-feldspar**, **quartz**, **chlorite**, albite.
3. Euhedral **quartz**, **epidote, Fe/Mg chlorite, calcite**, pyrite, fluorite, muscovite, (K-feldspar).
4. **Prehnite,** (fluorite).
5. 
   - **a. Calcite**, (fluorite, hematite).
   - **b.** Dark red/brown filling – **Adularia, Mg-chlorite** (also as ML-clay with Illite), **hematite** (quartz), (apatite); sometimes cataclastic.
   - **c. Calcite, adularia, laumontite, Mg-chlorite, quartz, illite** (also as ML-clay with chlorite), **hematite,** (albite).
6. **Calcite, adularia, Fe-chlorite, hematite, fluorite, quartz, pyrite**, **barite**, harmotome, REE-carbonate, apophyllite, gypsum, illite/chlorite (ML-clay), corrensite, chalcopyrite, galena, sphalerite, Ti-oxide, U-silicate, laumontite, Cu-oxide, sylvite, (Fe-oxyhydroxide), (Mg-chlorite), (apatite), (wolframite).
7. Calcite, pyrite.